Inorg. Chem. **2006**, *45*, 7144–7159

Targeted Guanine Oxidation by a Dinuclear Copper(II) Complex at Single Stranded/Double Stranded DNA Junctions

Lei Li,[†] Narasimha N. Murthy,[†,⊥] Joshua Telser,[||] Lev. N. Zakharov,[§] Glenn P. A. Yap,[§] Arnold L. Rheingold,[§,#] Kenneth D. Karlin,*[,†] and Steven E. Rokita*[,‡]

Department of Chemistry, The Johns Hopkins University, Baltimore, Maryland 21218, Department of Chemistry and Biochemistry, University of Maryland, College Park, Maryland 20742, Department of Biological, Chemical, and Physical Sciences, Roosevelt University, Chicago, Illinois 60605, and Department of Chemistry, University of Delaware, Newark, Delaware 19716

Received April 7, 2006

A dinuclear copper(II) complex $[Cu^{II}_2(PD'O^-)(H_2O)_2](ClO_4)_3$ (**5**) with terminal Cu(II)–H_2O moieties and a Cu···Cu distance of 4.13 Å (X-ray structure) has been synthesized and characterized by EPR spectroscopy (ferromagnetic coupling observed) and cyclic voltammetry. Dizinc(II) and mononuclear copper(II) analogues $[Zn^{II}_2(PD'O^-)(H_2O)_2]^{3+}$ (**7**) and $[Cu^{II}(mPD'OH)(H_2O)]^{2+}$ (**6**), respectively, have also been synthesized and structurally characterized. Reacting **5**/MPA/O_2 (MPA = 3-mercaptopropionic acid) with DNA leads to a highly specific oxidation of guanine (G) at a junction between single- and double-stranded DNA. Mass spectrometric analysis of the major products indicates a gain of +18 and +34 amu relative to initial DNA strands. The most efficient reaction requires G at the first and second unpaired positions of each strand extending from the junction. Less reaction is observed for analogous targets in which the G cluster is farther from the junction or contains less than four Gs. Consistent with our previous systems, the multinuclear copper center is required for selective reaction; mononuclear complex **6** is not effective. Hydrogen peroxide as a substitute for MPA/O_2 also does not lead to activity. Structural analysis of a $[Cu^{II}_2(PD'O^-)(G)]^{3+}$ complex (**8**) and dizinc analogue $[Zn^{II}_2(PD'O^-)(G)](ClO_4)_3$ (**9**) (G = guanosine) reveals coordination of the G O6 and N7 atoms with the two copper (or zinc) centers and suggests that copper–G coordination likely plays a role in recognition of the DNA target. The Cu_2–O_2 intermediate responsible for guanine oxidation appears to be different from that responsible for direct-strand scission induced by other multinuclear copper complexes; the likely course of reaction is discussed.

Introduction

The past decade has seen a proliferation of studies on DNA reaction induced by transition-metal complexes.[1−3] New species with an ability to cleave DNA strands are continually being discovered,[4−8] and more established species such as copper−phenanthroline $[Cu^{II}(OP)_2]^{2+}$ have remained the focus of mechanistic investigation and biological application.[9−12] The majority of complexes typically oxidize the

* To whom correspondence should be addressed. E-mail: rokita@umd.edu (S.E.R.); karlin@jhu.edu (K.D.K.).
[†] The Johns Hopkins University.
[⊥] Current address: Department of Chemistry, Indian Institute of Technology Madras, Madras 600 036, India.
[||] Roosevelt University.
[§] University of Delaware.
[#] Current address: Department of Chemistry and Biochemistry, University of California San Diego, La Jolla, CA 92093.
[‡] University of Maryland.

(1) O'Neill, M. A.; Barton, J. K. *Top Curr. Chem.* **2004**, *236*, 67−115.
(2) Cowan, J. A. *Curr. Opin. Chem. Biol.* **2001**, *5*, 634−642.
(3) Sigman, D. S.; Landgraf, R.; Perrin, D. M.; Pearson, L. *Met. Ions Biol. Syst.* **1996**, *33*, 485−513.
(4) Jin, Y.; Cowan, J. A. *J. Am. Chem. Soc.* **2005**, *127*, 8408−8415.
(5) Boll, I.; Kramer, R.; Brunner, J.; Mokhir, A. *J. Am. Chem. Soc.* **2005**, *127*, 7849−7856.
(6) Sissi, C.; Mancin, F.; Gatos, M.; Palumbo, M.; Tecilla, P.; Tonellato, U. *Inorg. Chem.* **2005**, *44*, 2310−2317.
(7) Patra, A. K.; Dhar, S.; Nethaji, M.; Chakravarty, A. R. *Dalton Trans.* **2005**, 896−902.
(8) Fang, Y. Y.; Claussen, C. A.; Lipkowitz, K. B.; Long, E. C. *J. Am. Chem. Soc.* **2006**, *128*, 3198−3207.
(9) Hirohama, T.; Kuranuki, Y.; Ebina, E.; Sugizaki, T.; Arii, H.; Chikira, M.; Selvi, P. T.; Palaniandavar, M. *J. Inorg. Biochem.* **2005**, *99*, 1205−1219.
(10) Zaid, A.; Sun, J. S.; Nguyen, C. H.; Bisagni, E.; Garestier, T.; Grierson, D. S.; Zain, R. *Chembiochem* **2004**, *5*, 1550−1557.
(11) Oyoshi, T.; Sugiyama, H. *J. Am. Chem. Soc.* **2000**, *122*, 6313−6314.
(12) Bales, B. C.; Pitie, M.; Meunier, B.; Greenberg, M. M. *J. Am. Chem. Soc.* **2002**, *124*, 9062−9063.

10.1021/ic0605930 CCC: $33.50 © 2006 American Chemical Society
Published on Web 08/10/2006

Chart 1

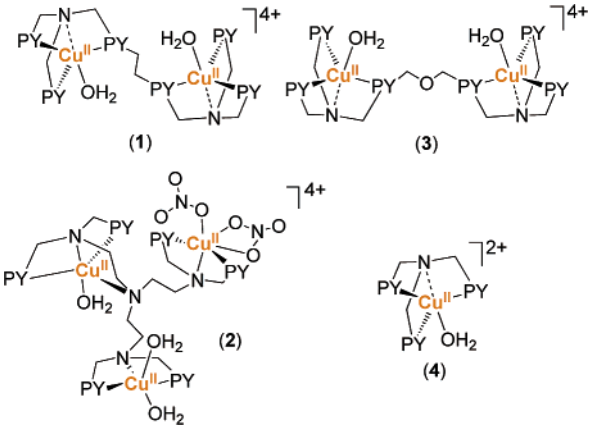

DNA backbone without sequence selectivity and thus create a complex array of DNA fragments. To achieve targeted strand scission, reagents such as Fe(II)−EDTA or $[Cu^{II}(OP)_2]^{2+}$ have been conjugated to compounds that direct their association with DNA.[13−17] In a complementary manner, ligands surrounding the metal can be modified to alter the type of chemistry that is promoted by the metal.[18,19] Future success in designing a broad platform of complexes exhibiting predictable chemio- and regiospecificity in reactions with nucleic acids depends on our ability to understand the determinants controlling the diverse activities of many existing examples.

Certain multinuclear copper complexes that were originally developed to model metalloenzymes[20] have also demonstrated a potent and selective ability to cleave the backbone of DNA by oxidation. Two species in particular, $[Cu^{II}_2(D^1)(H_2O)_2]^{4+}$ (**1**) and $[Cu^{II}_3(TP1)(H_2O)_3(NO_3)_2]^{4+}$ (**2**) (Chart 1), promote strand scission at junctions of single- and double-stranded (ss/ds) DNA with exquisite sensitivity to the nucleotide sequence.[21−23] Site specificity derives in part by the coordination of at least one copper to a guanine (G)-rich region,[24] and the subsequent chemistry depends on the ligand structure. The addition of only one more spacer atom linking the individual binding sites of copper in the dinuclear compound $[Cu^{II}_2(D^1)(H_2O)_2]^{4+}$(**1**) to generate the complex

Chart 2

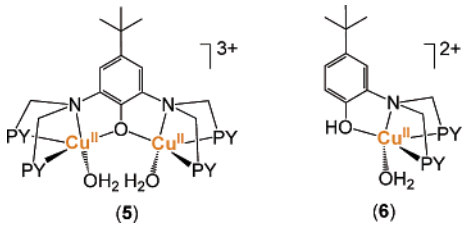

Chart 3

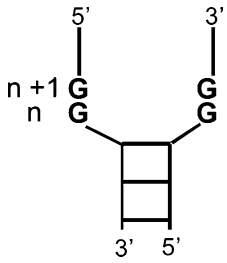

$[Cu^{II}_2(DO)(Cl)_2]^{2+}$ (**3**) was sufficient to abolish the selective strand scission of DNA.[21] Activities observed for di- and trinuclear complexes were furthermore not mimicked by their mononuclear analogues such as $[Cu^{II}(TMPA)(H_2O)]^{2+}$ (**4**), implying that DNA cleavage occurs via a multi-metal-mediated reaction.[21,22]

An alternative dinuclear copper complex $[Cu^{II}_2(PD'O^-)(H_2O)_2]^{3+}$ (**5**) (Chart 2) was described in a preliminary report to promote reaction at purine-rich junctions of ss/ds DNA in analogy to the other multinuclear copper complexes.[25] However, the oxidation promoted by **5** is unique to these multinuclear copper complexes. The presence of 3-mercaptopropionic acid (MPA) and ambient concentrations of O_2 did not support strand scission, as evident with **1** and **2**. Instead, these conditions resulted in the oxidation of G to 2,6-diamino-5-formamidino-4-hydroxypyrimidine (FAPy-G) as a major product with **5**. The synthesis and physical properties of this complex and its reactivity with DNA are now described in a more comprehensive manner. The crystal structures of **5** in the presence and absence of guanine have also been characterized, and its solid-state and solution properties are compared to related phenoxo-bridged dinuclear copper(II) complexes.

The initial DNA target used to characterize the reactivity of **5** contained four Gs distributed at the *n* and *n* + 1 position of the single-stranded DNA directly extended from the duplex region as illustrated in Chart 3. This was chosen as a likely target of oxidation by a multinuclear complex on the basis of our previous experience with such complexes. Now, the roles of the ss/ds junction and the proximal guanines have been investigated independently. Additionally, the mechanism of reaction has been examined for its dependence on molecular oxygen, sensitivity to quenching agents, response to H_2O_2 and thiols, product formation, and the activity of $[Cu^{II}(mPD'OH)(H_2O)]^{2+}$ (**6**), a newly prepared mononuclear analogue of **5**.

(13) Chen, C. H. B.; Gorin, M. B.; Sigman, D. S. *Proc. Natl. Acad. Sci. U.S.A.* **1993**, *90*, 4206−4210.
(14) Schultz, P. G.; Dervan, P. B. *J. Am. Chem. Soc.* **1983**, *105*, 7748−7750.
(15) Schultz, P. G.; Dervan, P. B. *Proc. Natl. Acad. Sci. U.S.A.* **1983**, *80*, 6834−6837.
(16) Sigman, D. S.; Chen, C. B.; Gorin, M. B. *Nature* **1993**, *363*, 474−475.
(17) Datwyler, S. A.; Meares, C. F. In *Probing of Proteins by Metal Ions and Their Low-Molecular-Weight Complexes*; Marcel Dekker: New York, 2001; Vol. 38, pp 213−254.
(18) Thorp, H. H. *Adv. Inorg. Chem.* **1995**, *43*, 127−177.
(19) Burrows, C. J.; Muller, J. G. *Chem. Rev.* **1998**, *98*, 1109−1151.
(20) Hatcher, L. Q.; Karlin, K. D. *J. Biol. Inorg. Chem.* **2004**, *9*, 669−683.
(21) Humphreys, K. J.; Karlin, K. D.; Rokita, S. E. *J. Am. Chem. Soc.* **2002**, *124*, 6009−6019.
(22) Humphreys, K. J.; Karlin, K. D.; Rokita, S. E. *J. Am. Chem. Soc.* **2002**, *124*, 8055−8066.
(23) Humphreys, K. J.; Karlin, K. D.; Rokita, S. E. *J. Am. Chem. Soc.* **2001**, *123*, 5588−5589.
(24) Ito, T.; Thyagarajan, S.; Karlin, K. D.; Rokita, S. E. *Chem. Commun.* **2005**, 4812−4814.
(25) Li, L.; Karlin, K. D.; Rokita, S. E. *J. Am. Chem. Soc.* **2005**, *127*, 520−521.

Experimental Section

General Materials. Oligodeoxynucleotides were purchased from Gibco BRL. T4 kinase and the appropriate buffer were obtained from New England Biolabs and [γ-^{32}P]ATP (3000 Ci/mmol) was obtained from Amersham. Solutions of the metal complexes and other reagents for strand scission were prepared fresh daily using distilled−deionized water (18 MΩ cm). Stock solutions of 3-mercaptopropionic acid (MPA, Aldrich), 2-mercaptoethanol (ME), and dithiothreitol (DTT) were titrated with Ellman's reagent to determine their free thiol concentration. All other chemicals were used as supplied by the manufacturer. UV−vis spectra were recorded with a Varian Cary-50 spectrophotometer. Elemental analyses were performed by Quantitative Technologies, Inc. (QTI, Whitehouse, NJ), and Desert Analytics (Tucson, AZ). ^{1}H NMR spectra were recorded at 300 MHz on a Bruker AMX-300 instrument. Chemical shifts were reported as δ values relative to an internal standard (Me_4Si) and the residual solvent proton.

PD′OH and [Cu$^{II}_2$(PD′O$^-$)(H$_2$O)$_2$](ClO$_4$)$_3$·3H$_2$O (5). The binucleating ligand PD′OH and its corresponding dicopper(II) complex, [Cu_2^{II}(PD′O$^-$)(H$_2$O)$_2$](ClO$_4$)$_3$·3H$_2$O, were synthesized according to published procedures.[25]

mPD′OH. 4-*tert*-Butyl-2-aminophenol (7.7 g, 46.6 mmol) was dissolved in 100 mL of methanol. Then, 2-picolyl chloride (12.9 g, 102 mmol) in degassed methanol (50 mL, bubbled with argon for 20 min) containing triethylamine (10.5 g, 103 mmol) was added dropwise. The resulting solution was stirred for 3 days at ∼65 °C under an argon atmosphere. The product mPD′OH was purified by column chromatography (silica gel). Elution with ethyl acetate removed the unreacted 2-picolyl chloride, and elution with ethyl acetate/hexane (1:1) yielded the desired product (13.2 g, 82%) as a brown-yellow solid (R_f = 0.21, silica gel, ethyl acetate:hexane = 1:1). ^{1}H NMR ($CDCl_3$, 300 MHz): δ 1.23 (s, 9H), 4.37 (s, 4H), 6.77−6.90 (m, 3H), 6.96−6.99 (m, 2H), 7.03−7.07 (m, 2H), 7.38−7.43 (m, 2H), 8.48−8.51 (m, 2H).

[Cu^{II}(mPD′OH)(H$_2$O)](ClO$_4$)$_2$·H$_2$O (6). A blue solution of **6** was obtained by the dropwise addition of 10 mL of an aqueous solution of Cu(ClO$_4$)$_2$·6H$_2$O (0.17 g, 0.44 mmol) to a 10 mL EtOH solution of mPD′OH (0.15 g, 0.44 mmol). Blue crystals (0.25 g, 78%) suitable for X-ray crystallographic analysis were obtained by the slow evaporation of this solution under reduced pressure. UV−vis (acetone): 450 nm (sh, 50 $M^{-1}cm^{-1}$), 677 nm (75 $M^{-1}cm^{-1}$). Anal. Calcd for ($C_{22}H_{29}Cl_2CuN_3O_{11}$): C, 40.91; H, 4.53; N, 6.51. Found: C, 40.98; H, 4.36; N, 6.41.

[Zn$^{II}_2$(PD′O$^-$)(H$_2$O)$_2$](ClO$_4$)$_3$·3H$_2$O (7). A degassed ethanol solution (8 mL, bubbled with argon for 20 min) of PD′OH (109 mg, 2 mmol) was mixed with a degassed aqueous solution (8 mL, bubbled with argon for 20 min) of Zn(ClO$_4$)$_2$·6H$_2$O (149 mg, 4 mmol) under an argon atmosphere and ambient temperature. A clear, light yellow solution formed, and yellow crystalline needles (205 mg, 80%) suitable for X-ray analysis were obtained from this by slow evaporation. ^{1}H NMR (CD_3OD, 300 MHz): δ 1.23 (s, 9H), 4.37 (s, 8H), 6.77−6.90 (m, 3H), 6.96−6.99 (m, 2H), 7.03−7.07 (m, 2H), 7.38−7.43 (m, 2H), 8.48−8.51 (m, 2H). Anal. Calcd for ($C_{34}H_{39}Zn_2N_6O_{15}$)·3H$_2$O: C, 39.77; H, 4.02; N, 8.18. Found: C, 39.34; H, 3.79; N, 7.98.

[Cu$^{II}_2$(PD′O$^-$)(guanosine)](ClO$_4$)$_3$·6H$_2$O (8). A MeOH solution (10 mL) of **5** (60 mg, 0.059 mmol) was mixed with a 15 mL MeOH solution of guanosine (17 mg, 0.06 mmol). After stirring for ∼0.5 h under ambient temperature, we observed a clear green solution. The addition of 100 mL of Et$_2$O to this solution yielded a light green powder (62 mg, 76%). A single crystal suitable for X-ray crystallographic analysis was obtained by recrystallization of this green powder in MeOH/Et$_2$O. UV−vis (acetone): 385 nm (sh, 600 M^{-1} cm^{-1}), 690 nm (160 M^{-1} cm^{-1}). Anal. Calcd for ($C_{44}H_{48}Cl_3Cu_2N_{11}O_{18}$)·6H$_2$O: C, 38.85; H, 4.45; N, 11.33. Found: C, 38.67; H, 4.01; N, 11.40.

[Zn$^{II}_2$(PD′O$^-$)(guanosine)](ClO$_4$)$_3$·5H$_2$O (9). A MeOH solution (10 mL) of **7** (90 mg, 0.094 mmol) was mixed with a 15 mL MeOH solution of guanosine (28 mg, 0.1 mmol). A clear yellow solution was obtained after stirring for ∼0.5 h under ambient temperature. The addition of 100 mL of Et$_2$O to this solution yielded a yellow powder (102 mg, 81%). A single crystal suitable for X-ray crystallographic analysis was obtained by recrystallization of this powder in MeOH/Et$_2$O. Anal. Calcd for ($C_{44}H_{48}Cl_3Cu_2N_{11}O_{18}$)·5H$_2$O: C, 39.26; H, 4.34; N, 11.45. Found: C, 39.17; H, 4.00; N, 11.14.

Electrochemistry. Cyclic voltammetry was carried out with a Bioanalytical Systems BAS-100B electrochemical analyzer. The cell was a standard three-electrode system with a platinum wire auxiliary as the counter electrode. A glassy carbon electrode (GCE, BAS MF 2012) was used as the working electrode and saturated calomel as reference electrode. The measurements were performed at room temperature in DMF containing 0.1 M tetrabutylammonium hexafluorophosphate (TBAHP) and either the copper or zinc complex (1−0.1 mM). The solvent was deoxygenated by bubbling argon through the solution.

EPR Spectroscopy and Simulations of Copper Complexes. Electron paramagnetic resonance (EPR) spectra were recorded on a Bruker EMX spectrometer controlled with a Bruker ER 041 X G microwave bridge operating at the X-band (∼9.4 GHz) at room temperature and in the 30−77 K range. The low-temperature EPR measurements were carried out via either a continuous-flow liquid-helium cryostat and ITC503 temperature controller made by Oxford Instruments, Inc., or a liquid-nitrogen finger dewar. EPR spectra were recorded for 1:1 DMF:toluene solutions of **5** and **6** at 34 K; experimental conditions are given in the relevant figure captions. Computer simulations of EPR spectra were performed using the g77 FORTRAN program DDPOWJHE, available from J. Telser. This program has been employed previously for a dinuclear Mn(II) system.[26] DDPOWJHE uses as a basis set a system of two electronic spins (S_1, S_2), each coupled to two nuclear spins (I_1, I_2). For the dinuclear complex **5**, $S_1 = S_2 = 1/2$, $I_1 = I_2 = 3/2$ is used, along with an approximation of 100% ^{63}Cu. Effects of the natural isotopic abundance of ^{63,65}Cu is masked by the EPR line width in solution. For the mononuclear complex **6**, $S_1 = 1/2$, $S_2 = 0$, $I_1 = 3/2$, $I_2 = 0$. A standard spin Hamiltonian for a coupled spin system was employed[27] that includes, in order of increasing interaction energy, isotropic nuclear Zeeman coupling to each ^{63}Cu nucleus, anisotropic hyperfine coupling between each ^{63}Cu nucleus and each Cu(II) electronic spin, anisotropic electronic Zeeman coupling to each Cu(II) spin, and anisotropic exchange coupling between the two electronic spins

$$H = S_1 \cdot \boldsymbol{J} \cdot S_2 + \sum [\beta B \cdot g_i \cdot S_i + S_i \cdot A_i \cdot I_i + \beta_N g_N B \cdot I_i \, (i = 1, 2)] \quad (1)$$

The electron spin−electron spin coupling can be separated into an isotropic (Heisenberg−Dirac−van Vleck) exchange interaction scalar, J, and an anisotropic, dipolar interaction matrix, $\boldsymbol{D}$

$$H_{exch} = JS_1 \cdot S_2 + S_1 \cdot \boldsymbol{D} \cdot S_2,$$
$$\text{where } D_x = -D/3 + E,\ D_y = -D/3 - E,\ D_z = (2/3)D$$

(26) Howard, T.; Telser, J.; DeRose, V. J. *Inorg. Chem.* **2000**, *39*, 3379−3385.
(27) Abragam, A.; Bleaney, B. *Electron Paramagnetic Resonance of Transition Ions*; Dover Publications: New York, 1986.

where D is the axial term in the spin−spin dipolar interaction and E is the rhombic term in this interaction. These definitions are analogous to those for single-ion second-rank zero-field splitting,[27] the effects of which need not be considered for dinuclear Cu(II) $S_i = 1/2$, in contrast to $S_i = 5/2$ for Mn(II).[26]

The program DDPOWJHE (using EISPACK software) diagonalizes the entire 64 × 64 (for $S_1 = S_2 = 1/2$, $I_1 = I_2 = 3/2$) spin Hamiltonian matrix to provide eigenvalues and eigenvectors, from which the EPR transition energies and magnetic-dipole-allowed transition probabilities are calculated in the standard way. An EPR powder pattern is generated by an "igloo" method.[28]

Purification and Labeling of DNA. Oligodeoxynucleotides were purified prior to use by denaturing (7 M urea) polyacrylamide gel electrophoresis and elution into 50 mM NaOAc and 1 mM EDTA (pH 5.2). The resulting solution was extracted with phenol/chloroform. DNA was then precipitated by the addition of 3 M NaOAc and 95% ethanol, dried under reduced pressure, and redissolved in water. Concentrations were determined by absorption at 260 nm and the extinction coefficients provided by the manufacturer. DNA was radiolabeled by incubation with [γ-^{32}P]-ATP and T4 kinase according to protocols provided by the supplier. The 5′-^{32}P-labeled DNA was isolated by passage over a Micro-BioSpin P-6 column (Bio-Rad). Duplex structures containing ss/ds junctions were formed by annealing a 5′-^{32}P-labeled oligodeoxynucleotide (100 nM, 90 nCi) and its (partially) complementary sequence (200 nM) in sodium phosphate (10 mM, pH 7.5) by heating to 95 °C followed by slow cooling to room temperature.

DNA Oxidation by Copper Complexes. Various concentrations of the dinuclear complex $[Cu_2^{II}(PD'O^-)(H_2O)_2](ClO_4)_3 \cdot 2H_2O$ (**5**) or its mononuclear analogue $[Cu^{II}(mPD'OH)(H_2O)](ClO_4)_2 \cdot H_2O$ (**6**) were combined with labeled DNA samples (100 nM, 90 nCi) in sodium phosphate (10 mM, pH 7.5), and the reaction was initiated by the addition of 5 μL of MPA (5 mM) to yield a total volume of 50 μL. Reaction was quenched after incubation for 15 min under ambient temperature by the addition of 10 mM diethyl dithiocarbamic acid (5 μL). The DNA was isolated by ethanol precipitation and dried under high vacuum. As indicated, certain samples were further treated with 20 μL of piperidine (0.2 M) for 30 min at 90 °C. These samples were dried under reduced pressure, twice redissolved with 20 μL of water, and subsequently dried to remove trace quantities of piperidine. The isolated DNA was re-suspended in 10 μL of water, normalized to 45 nCi per sample, and mixed with 3 μL of loading buffer (0.25% bromphenol blue, 0.25% xylene cyanole, 3% sucrose, and 7 M urea). These samples were then analyzed by denaturing (7 M urea) polyacrylamide (20%) gel electrophoresis and visualized by autoradiography and PhosphorImagery (Molecular Dynamics). Product profiles were quantified with ImageQuant and ImageJ software.

O_2 Dependence of the Reaction by Multinuclear Copper Complex 5. A solution containing target DNA (100 nM) and 100 μM $[Cu^{II}_2(PD'O^-)(H_2O)_2](ClO_4)_3 \cdot 2H_2O$ (**5**) was degassed by bubbling with prepurified nitrogen using a syringe needle for 15 min prior to reaction initiated by the addition of 5 μL of MPA (5 mM, not degassed). The reaction mixture was blanketed with nitrogen gas over a 15 min incubation. Product analysis then followed the standard procedures described above.

DNA Reaction in the Presence of H_2O_2 and Complex 5. $[Cu_2^{II}(PD'O^-)(H_2O)_2](ClO_4)_3 \cdot 2H_2O$ (**5**, 5 μL of a 1 mM solution) was combined with labeled DNA samples (100 nM, 90 nCi) in sodium phosphate buffer (10 mM, pH 7.5), and strand scission was initiated by the addition of 5 μL of H_2O_2 (5 mM) to yield a total volume of 50 μL. Product analysis followed the standard procedures described above.

Scheme 1

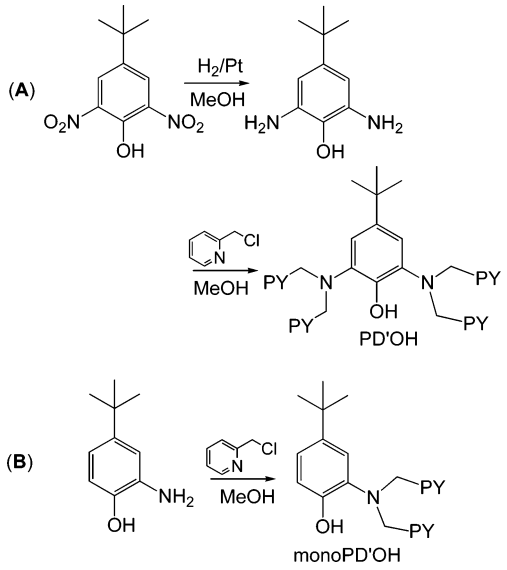

Reaction Between DNA and Complex 5 in the Presence of Radical Scavengers. The quenching agents (10 mM), ethanol, D-mannitol, and *tert*-butyl alcohol, were alternatively added to standard reaction mixtures of DNA and **5**. The reaction was again initiated with MPA, quenched, and analyzed as described above.

HPLC and ESI/MS Analysis. Reaction mixtures (10−30 nmol DNA) were separated by reverse phase HPLC, (C-18, Varian Microsorb-MV, 300 Å pore, 250 mm) using a gradient (60 min, 1 mL/min) of 5−18% acetonitrile in aqueous triethylammonium acetate (10 mM, pH 6.5) as controlled by a Jasco PU-980 system (Jasco, Easton, MD). Individual products were manually collected, lyophilized, and then redissolved in 5 M ammonium acetate. This solution was incubated for 3 h under ambient temperature before ethanol was added to precipitate the DNA at −80 °C. The process of dissolving, lyophilizing, and precipitating the DNA was repeated six times. Samples were then analyzed by nanospray ionization mass spectroscopy (NSI-MS, Thermo Finnigan LCQ, University of Maryland, Mass Spectroscopic facility) using direct injection with an applied voltage of −1.0 kV and a capillary temperature of 150 °C.

Results

(1) Synthesis and Characterizations of Cu and Zn Complexes. Synthesis of Metal Complexes. The symmetrical binucleating ligand PD′OH was synthesized in two steps as shown in Scheme 1. The product of the first step, 4-*tert*-butyl-2,6-diaminophenol (Scheme 1, A), was not stable in air; thus, its synthesis was carried out under an argon atmosphere. Reaction of commercial 2-amino-4-*tert*-butylphenol with 2 equiv of picoyl chloride gave the mononuclear analogue mPD′OH (Scheme 1, B).

Copper(II) complexes $[Cu^{II}_2(PD'O^-)(H_2O)_2](ClO_4)_3$ (**5**)[25] and $[Cu^{II}(mPD'OH)(H_2O)](ClO_4)_2$ (**6**) were synthesized by mixing the appropriate ligand with 2 and 1 equiv of $Cu(ClO_4)_2 \cdot 6H_2O$, respectively. Both compounds are relatively stable as solids. However, solutions of **5** changed from green to reddish brown over several days. The copper(II) centers

(28) Mombourquette, M. J.; Weil, J. A. *J. Magn. Reson.* **1992**, *99*, 37−44.

most likely promote slow oxidation of its ligand, because solutions of the analogous dizinc analogue $[Zn^{II}_2(PD'O^-)(H_2O)_2](ClO_4)_3$ (**7**) appear unchanged under the same condition. All solutions of copper complexes were prepared fresh daily for the studies described below.

X-ray Structural Analysis of $[Cu^{II}_2(PD'O^-)(H_2O)_2]^{3+}$ (5), $[Cu^{II}(mPD'OH)(H_2O)]^{2+}$ (6), and $[Zn^{II}_2(PD'O^-)(H_2O)_2]^{3+}$ (7). Perspective views of the cationic portion of complexes **5**−**7,** along with **8** and **9** (discussed below) are shown in Figures 1−4.[29] Crystal and refinement data and selective bond distances and angles are all given in the Supporting Information. The structure of **5** (Figure 1) consists of two crystallographically independent moieties with very similar Cu(II) coordination environments. The copper atoms are bound by a bridgehead amine and two nitrogen atoms from the pyridyl ligand donors. The endogenous bridging phenolate (O1) and an exogenous water molecule (O2) complete the penta-coordination. The geometry around each copper can be described as being slightly distorted square pyramidal, with the phenolate (O1) occupying the axial position of both copper(II) ions, each possessing a $N3(O_{H_2O})$ basal plane. Structural analysis of $[Cu^{II}_2(PD'O^-)(H_2O)_2]^{3+}$ (**5**) by the method defined by Reedijk and Addison reveals a $\tau = 0.09$ for each copper atom, where $\tau = 0.0$ represents a perfect square pyramid (SP) and $\tau = 1$ represents a perfect trigonal bipyramidal (TBP) geometry.[30] This τ value (Table 1) compares very well with those determined from related complexes $([Cu^{II}_2(PDO^-)(^-OMe)_2]^+$, $[Cu^{II}_2(PDO^-)(^-HCO_2)]^{2+}$, $[Cu^{II}_2(XYL-O^-)(^-OH)]^{2+}$, and $[Cu^{II}_2(UN-O^-)(^-OH)]^{2+}$) (Chart 4), indicating that this slightly distorted SP copper(II) coordination geometry is favored with these dinucleating ligands containing phenolate.[31−33] However, the phenoxo oxygen atom in **5** occupies the axial position, whereas in the other four complexes, one of the pyridyl nitrogen atom fills this role. Probably, the "short" pyridyl methyl arms and the altered juxtaposition of the donor groups in the $PD'O^-$ framework (compared to longer-armed chelates in the other complexes, Chart 4) causes the change in position of axial vs equatorial ligands.

The structure of $[Cu^{II}_2(PD'O^-)(H_2O)_2]^{3+}$ (**5**) can be further described by delineating three planes. The central plane is defined by the phenol ring of this binucleating ligand and further extended by the in-plane phenolate oxygen atom, the two copper ions, and the two bridgehead amino nitrogen atoms. (A and B of Figure 1). The other two planes are defined by the tridentate dipicolylamine (PY1) moieties, because each chelating tridentate group possesses two pyridyl units that are nearly coplanar. Thus, the copper(II) ion lies very close to the plane established by the two pyridyl groups, whereas the amino nitrogen is ∼0.4 Å above this plane and the coordinated water oxygen is ∼0.8 Å below this (Figure 1A). The dihedral angle between the central plane and each PY1 plane is 98.2°, indicating that they are almost perpendicular to each other. The dihedral angle between the two PY1 planes is 45.6°.

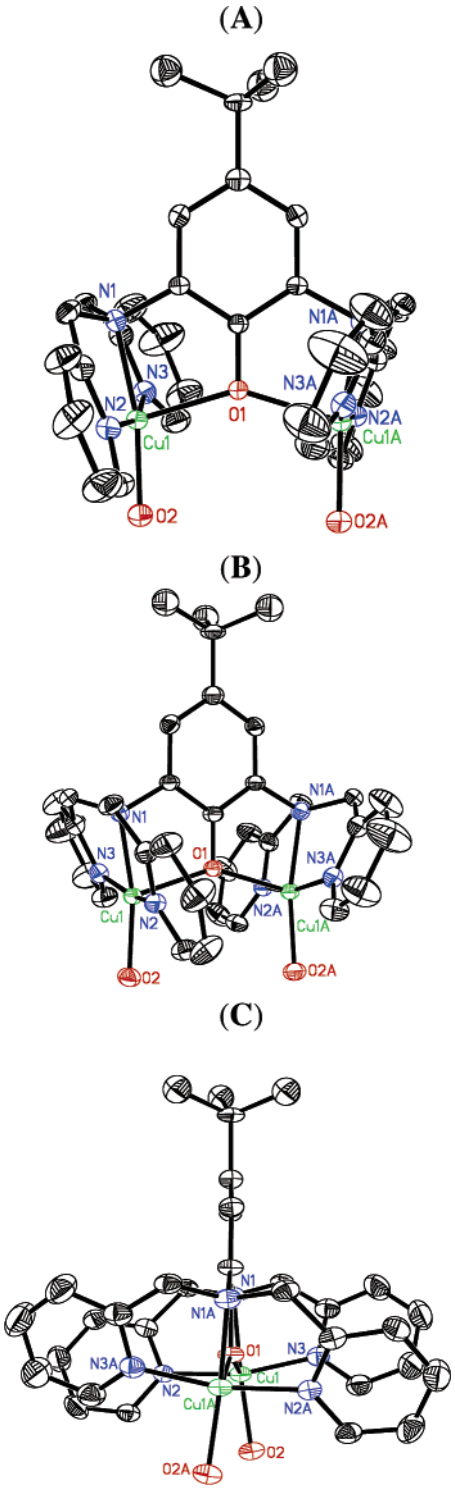

Figure 1. ORTEP views of the structure of the cationic portion of $[Cu^{II}_2(PD'O^-)(H_2O)_2]^{3+}$ (**5**) with selected distances: (A) view from the angle perpendicular to the phenolate plane; (B) rotated ∼30° from the position of view A; (C) rotated 90° from the position of view A. Cu(1)−O(1) = 2.1519(12) Å, Cu(1)−O(2) = 1.977(3) Å, Cu(1)−N(1) = 2.043(4) Å, Cu(1)−N(2) = 2.000(4) Å, Cu(1)−N(3) = 2.000(4) Å, Cu(1)···Cu(2) = 4.13 Å.[29]

(29) See the Supporting Information.
(30) Addison, A. W.; Rao, T. N.; Reedijk, J.; Vanrijn, J.; Verschoor, G. C. *J. Chem. Soc., Dalton Trans.* **1984**, 1349−1356.
(31) Murthy, N. N.; Mahroof-Tahir, M.; Karlin, K. D. *Inorg. Chem.* **2001**, *40*, 628−635.
(32) Karlin, K. D.; Hayes, J. C.; Gultneh, Y.; Cruse, R. W.; Mckown, J. W.; Hutchinson, J. P.; Zubieta, J. *J. Am. Chem. Soc.* **1984**, *106*, 2121−2128.
(33) Murthy, N. N.; Mahroof-Tahir, M.; Karlin, K. D. *J. Am. Chem. Soc.* **1993**, *115*, 10404−10405.

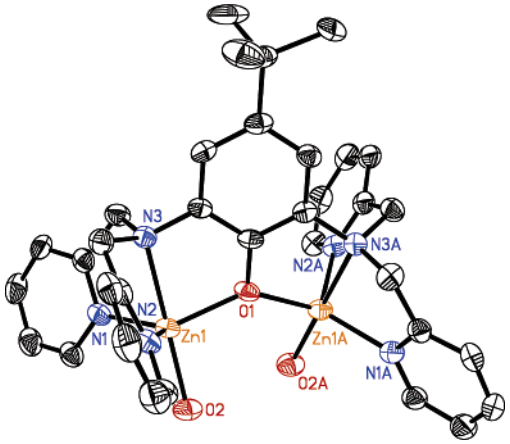

Figure 2. ORTEP views of the structure of the cationic portion of $[Zn^{II}_2(PD'O^-)(H_2O)_2]^{3+}$ (**7**) with selected distances. Zn(1)−O(1) = 2.037-(2) Å, Zn(1)−O(2) = 2.004(3) Å, Zn(1)−N(1) = 2.066(3) Å, Zn(1)−N(2) = 2.050(3) Å, Zn(1)−N(3) = 2.196(3) Å, Zn(1A)−O1 = 2.034(2) Å, Zn-(1A)−O(O2A) = 2.000(3) Å, Zn(1A)−N(1A) = 2.069(3) Å, Zn(1A)−N(2A) = 2.050(3) Å, Zn(1A)−N(3A) = 2.195(3) Å, Zn(1)···Zn(1A) = 3.80 Å.[29]

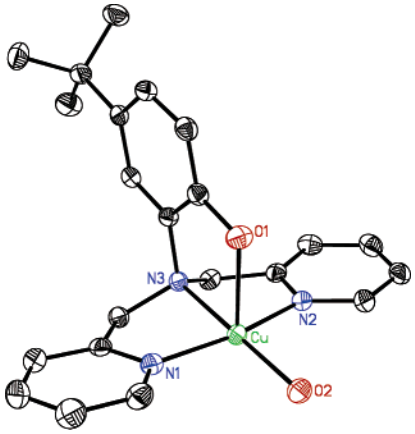

Figure 3. ORTEP views of the structure of the cationic portion of $[Cu^{II}(mPD'OH)(H_2O)]^{2+}$ (**6**) with selected distances. Cu−O(1) = 2.260(2) Å, Cu−O(2) = 1.980(2) Å, Cu−N(1) = 1.990(2) Å, Cu−N(2) = 2.000(2) Å, Cu−N(3) = 2.041(2) Å.[29]

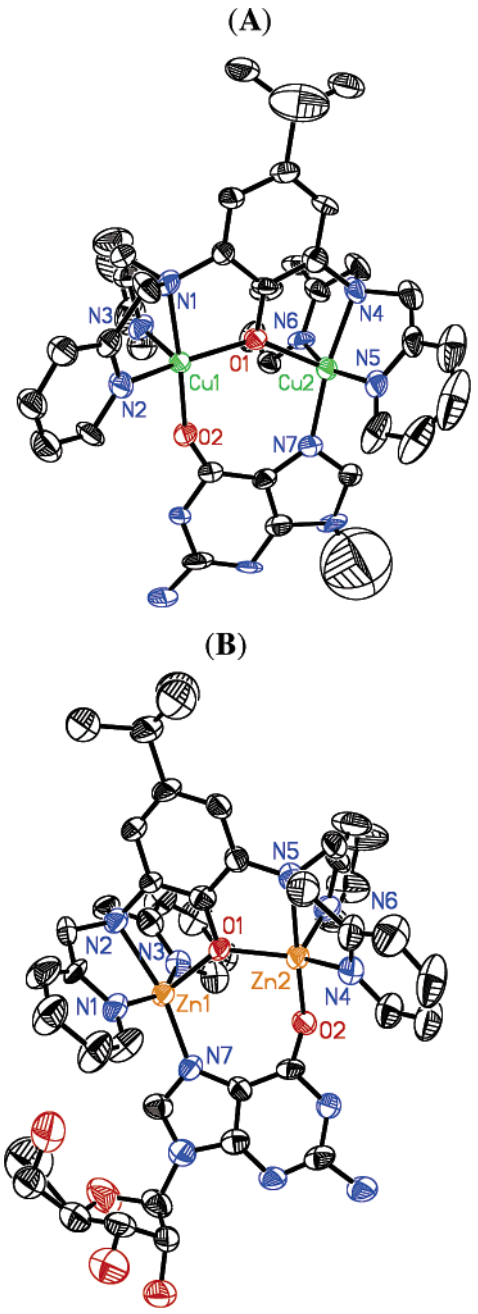

Figure 4. (A) ORTEP diagram showing the cationic portion of complex $[Cu^{II}_2(PD'O^-)(G)](ClO_4)_3$ (**8**, G = guanosine, the ribose entity is disordered) with selected distances. Cu1−O2 = 1.955(4) Å, Cu(2)−N7 = 1.990(5) Å, Cu(1)···Cu(2) = 3.81 Å.[29] (B) ORTEP diagram showing the cationic portion of complex $[Zn^{II}_2(PD'O^-)(G)](ClO_4)_3$ (**9**, G = guanosine) with selected distances. Zn(1)−N7 = 2.041(6) Å, Zn(2)−O2 = 1.997(4) Å, Zn(1)···Zn-(2) = 3.62 Å.[29] Normally/conventionally, the keto-oxygen that binds Cu^{II} or Zn^{II} in these structures is referred to as O6.

The τ value for the copper(II) ions in $[Cu^{II}_2(PD'O^-)(H_2O)_2]^{3+}$ (**5**) is almost identical to those in $[Cu^{II}_2(PDO^-)(^-OMe)_2]^+$, $[Cu^{II}_2(PDO^-)(^-HCO_2)]^{2+}$, $[Cu^{II}_2(XYL-O^-)(^-OH)]^{2+}$, and $[Cu^{II}_2(UN-O^-)(^-OH)]^{2+}$ (Table 1). However, only one central plane defined by the phenolate group can be used to describe the four latter compounds. Unlike **5**, all these complexes possess the bis[2-(2-pyridyl)ethyl]amine (PY2) moieties instead of PY1. The extra carbon of each chelate arm changes the nature of copper chelation (Chart 4). The Cu(II)···Cu(II) distances in these compounds (Table 1) are noteworthy. The largest Cu(II)···Cu(II) separation was found to be 4.13 Å in **5**, followed by 3.74 Å in $[Cu^{II}_2(PDO^-)(^-OMe)_2]^+$ and 3.65 Å in $[Cu^{II}_2(PDO^-)(^-HCO_2)]^{2+}$.[33] $[Cu^{II}_2(XYL-O^-)(^-OH)]^{2+}$ and $[Cu^{II}_2(UN-O^-)(^-OH)]^{2+}$ possess a Cu^{II}_2-μ-phenoxo-μ-hydroxo core and have short Cu-(II)...Cu(II) separations, 3.08 and 3.04 Å, respectively.[32,34] The significant elongation of the Cu···Cu distance in **5** likely results from the rigid nature of its ligand framework. In contrast to its structural analogues, the PD′OH ligand has no spacers between the amino nitrogen atoms and phenolate ring; in addition, its arms between the bridgehead amino nitrogens and pyridyl units are also shortened (i.e., they possess a one-methylene CH_2 vs a two-methylene CH_2CH_2 chelate arm). Both effects tend to force the copper(II) ions apart. Thus, **5** does not possess the second single-atom bridging unit such as the bridging hydroxyl group in its

(34) Nasir, M. S.; Karlin, K. D.; Mcgowty, D.; Zubieta, J. *J. Am. Chem. Soc.* **1991**, *113*, 698−700.

Table 1. Selected Structural Information of **5** and Its Analogues

complexes	M−M distance (Å)	τ	ref
$[Cu^{II}_2(PD'O^-)(H_2O)_2]^{3+}$ (**5**)	4.13	0.09	this work
$[Cu^{II}(mPD'OH)(H_2O)]^{2+}$ (**6**)		0.23	this work
$[Zn^{II}_2(PD'O^-)(H_2O)_2]^{3+}$ (**7**)	3.80	0.83, 0.86	this work
$[Cu^{II}_2(PDO^-)(^-OMe)_2]^{+}$	3.74	0.33	33
$[Cu^{II}_2(PDO^-)(^-HCO_2)]^{2+}$	3.65	0.28	33
$[Cu^{II}_2(XYL-O^-)(^-OH)]^{2+}$	3.08	0.07, 0.04	32
$[Cu^{II}_2(UN-O^-)(^-OH)]^{2+}$	3.04	0.05, 0.15	34
$[Cu^{II}_2(PD'O^-)(G)]^{3+}$ (**8**)	3.81	0.18, 0.50	this work
$[Zn^{II}_2(PD'O^-)(G)]^{3+}$ (**9**)	3.62	0.95, 0.81	this work

Chart 4

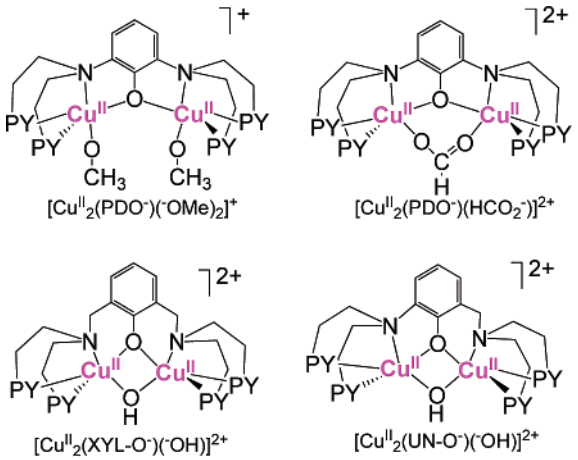

structural analogues.[32,34] Instead, each copper(II) ion acquires a water molecule as a fifth ligand.

A dizinc(II) analogue of $[Cu^{II}_2(PD'O^-)(H_2O)_2]^{3+}$ (**5**) was synthesized to compare and contrast a non-redox-active metal in the $PD'O^-$ ligand framework. Structure analysis reveals that $[Zn^{II}_2(PD'O^-)(H_2O)_2]^{3+}$ (**7**) remains a phenolate-bridged dinuclear center in which each zinc ion is pentacoordinated with a phenoxo oxygen, three nitrogen atoms from the PY1 unit, and exogenous water as ligands (Figure 2). However, the coordination geometry of the two zinc ions is no longer equivalent and also very different from that of the Cu(II) ions in **5**. Whereas the copper ions in **5** lie close to the plane defined by the amine atoms N3 and N3A and the phenoxo oxygen atom O1 of its phenolate (Figure 1), the zinc ions in **7** are displaced and on the opposite side of this plane by ∼0.55 Å (Figure 2). The τ values (0.83 and 0.86) for the zinc centers reveal slightly distorted TBP geometry, with the axial positions being occupied by the bridgehead nitrogen (N3, N3A) and exogenous water oxygen (O2, O2A) atoms. In fact, Zn(II) ions often favor trigonal bipyramidal geometry, whereas Cu(II) favors the SP geometries, which are both consistent with the structures observed here.[35,36] Finally, the Zn···Zn distance in **7** is 3.799 Å, about 0.2 Å shorter than the Cu...Cu distance in **5**.

The copper(II) ion coordination geometry of $[Cu^{II}(mPD'OH)(H_2O)]^{2+}$ (**6**), the mononuclear analogue of **5**, closely mimics its half structure (Figure 3). The planes defined by the central phenol and the PY1 group are still present. The dihedral angle between these is 90.8°, which is slightly smaller than that in **5**. However, the phenol group of **6** retains its hydrogen, unlike that for the bridging phenolate groups in binuclear complexes **5** or **7**. The pK_a value of phenol has been reported to decrease from 10.0 in free phenol to 9.2 when coordinated to a single Cu(II) ion;[37,38] thus, at neutral pH, or under the conditions of the synthesis and isolation of crystalline compound **6**, the phenolic proton stays associated.[39−42] The phenol pK_a is expected to decrease even more when an additional metal center binds and leads to deprotonation, as evident in the structures of **5**, **7**, and nearly all phenol(ate)−dicopper(II) complexes. The negative charge of the phenolate group in turn draws the positively charged metal ions closer, as evident by the ∼0.1 Å shorter Cu−$O_{phenolate}$ bond in dinuclear **5** compared to that (Cu−O_{phenol}) in **6**. The τ value for the copper(II) ion in **6** is found to be 0.23. Although this indicates a distorted SP geometry for copper(II) (more so than in **5**, with $\tau = 0.09$), the phenol oxygen atom occupies the axial position, as it does in $[Cu^{II}_2(PD'O^-)(H_2O)_2]^{3+}$ (**5**). Given the similar coordination environment for copper ions in **5** and **6**, we conclude that it is the longer Cu−O_{phenol} bond that triggers the copper geometry change from a near-perfect SP in **5** to a twisted one in **6**.

Coordination to Guanosine (G) in $[Cu^{II}_2(PD'O^-)(G)]^{3+}$ (8) and $[Zn^{II}_2(PD'O^-)(G)]^{3+}$ (9). To provide insight into the possible binding of $[Cu^{II}_2(PD'O^-)(H_2O)_2]^{3+}$ (**5**) to donors in DNA (in particular to guanine), we prepared complexes with guanosine $[Cu^{II}_2(PD'O^-)(G)]^{3+}$ (**8**) and its dizinc analogue $[Zn^{II}_2(PD'O^-)(G)]^{3+}$ (**9**). Although the ribose entity in $[Cu^{II}_2(PD'O^-)(G)]^{3+}$ (**8**) is disordered, its solid-state structure clearly shows that G bridges the copper centers via coordination to its O6 (labeled O2 in the X-ray structure) keto group and N7 (Figure 4A). Each copper ion in **8** remains pentacoordinated, as described earlier for $[Cu^{II}_2(PD'O^-)(H_2O)_2]^{3+}$ (**5**), but now guanosine replaces the water molecules as the exogenous fifth ligand. Because of the O6 (labeled O2 in the X-ray structure) or N7 coordination, the two copper ions in **8** are no longer equal. The τ values for the two copper ions are found to be 0.18 (N7 as chelate) and 0.50 (O6 (O2) as chelate), respectively, with the latter indicating a hybrid copper coordinating geometry of SP and TBP. The Cu···Cu distance is 3.81 Å in **8**, ∼0.22 Å shorter than that in **7**.

The dizinc(II) analogue $[Zn^{II}_2(PD'O^-)(G)]^{3+}$ (**9**) formed under the same conditions used to generate $[Cu^{II}_2(PD'O^-)(G)]^{3+}$ (**8**) and was found to possess a similar bridging structure containing O6 (labeled O2 in the X-ray structure) and N7 of guanosine and the dizinc center (Figure

(35) Ohtsu, H.; Shimazaki, Y.; Odani, A.; Yamauchi, O.; Mori, W.; Itoh, S.; Fukuzumi, S. *J. Am. Chem. Soc.* **2000**, *122*, 5733−5741.
(36) Canary, J. W.; Allen, C. S.; Castagnetto, J. M.; Chiu, Y. H.; Toscano, P. J.; Wang, Y. H. *Inorg. Chem.* **1998**, *37*, 6255−6262.
(37) Masuda, H.; Odani, A.; Yamauchi, O. *Inorg. Chem.* **1989**, *28*, 624−625.
(38) Kiss, T.; Szucs, Z. *J. Chem. Soc., Dalton Trans.* **1986**, 2443−2447.
(39) Sarkar, S.; Mondal, A.; Ribas, J.; Drew, M. G. B.; Pramanik, K.; Rajak, K. K. *Eur. J. Inorg. Chem.* **2004**, 4633−4639.
(40) de Oliveira, M. C. B.; Scarpellini, M.; Neves, A.; Terenzi, H.; Bortoluzzi, A. J.; Szpoganics, B.; Greatti, A.; Mangrich, A. S.; de Souza, E. M.; Fernandez, P. M.; Soares, M. R. *Inorg. Chem.* **2005**, *44*, 921−929.
(41) Shimazaki, Y.; Huth, S.; Hirota, S.; Yamauchi, O. *B Chem. Soc. Jpn.* **2000**, *73*, 1187−1195.
(42) Ito, S.; Nishino, S.; Itoh, H.; Ohba, S.; Nishida, Y. *Polyhedron* **1998**, *17*, 1637−1642.

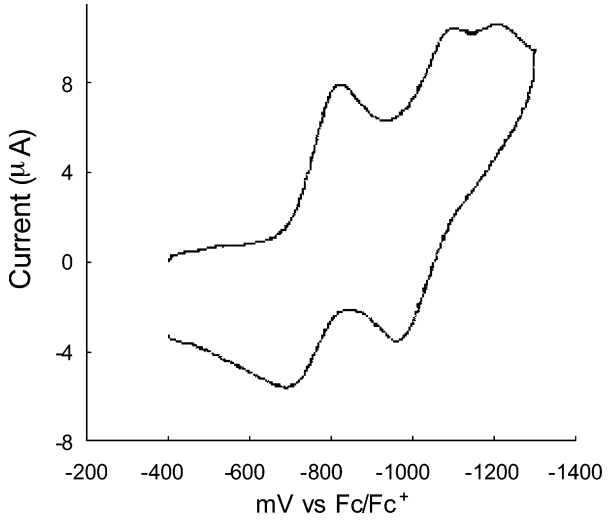

Figure 5. Cyclic voltammogram of compound $[Cu^{II}_2(PD'O^-)(H_2O)_2]^{3+}$ (**5**) (1 mM) in DMF under an inert atmosphere. Scan rate = 0.1 V/s; supporting electrolyte was 0.1 M TBAHP (tetrabutylammonium hexafluorophosphate).

4B). In this example, the ribose moiety is also clearly resolved. The zinc ions in **9** possess nearly perfect TBP geometry, as indicated by τ values of 0.95 and 0.80, respectively (Table 1).[29] These values are also quite similar to those of $[Zn^{II}_2(PD'O^-)(H_2O)_2]^{3+}$ (**7**). The Zn···Zn distance in **9** is even shorter (3.62 Å) than the Zn···Zn distance in **7** (3.80 Å) and Cu···Cu distance in **8** (3.81 Å), suggesting that the bridging guanosine again brings the dizinc centers close.

Electrochemistry. The electrochemical behavior of $[Cu^{II}_2(PD'O^-)(H_2O)_2]^{3+}$ (**5**) was investigated in DMF under an inert atmosphere. The CV of **5** is characterized by two successive, one-electron quasireversible electrochemical processes (Figure 5). The first ($E_{1/2} = -0.76$ V vs Fc/Fc^+) can be assigned to a $Cu^{II}Cu^{II}/Cu^{II}Cu^{I}$ redox couple, and the second ($E_{1/2} = -1.03$ V) corresponds to a subsequent Cu^{II}-$Cu^{I}/Cu^{I}Cu^{I}$ redox process.[43,44] (Note: the extra peak beyond the second reduction may result from absorption of the mixed-valence form to the electrode surface, or possibly further reduction of the dicopper(I) form to Cu^0).[47]

The phenolate group may also be oxidized to give a Cu(II)-coupled phenoxo radical ($Cu(II)_2-^{\bullet}OAr$). However, such oxidations usually occur at more positive potentials,[43−47] and no redox process could be detected for **5** in the more positive potential region. To supplement this conclusion, we also examined the redox behavior of dizinc analogue $[Zn^{II}_2(PD'O^-)(H_2O)_2]^{3+}$ (**7**). As expected, no redox process was observed within the −1.6 to +0.4 V (vs Fc/Fc^+) potential window,

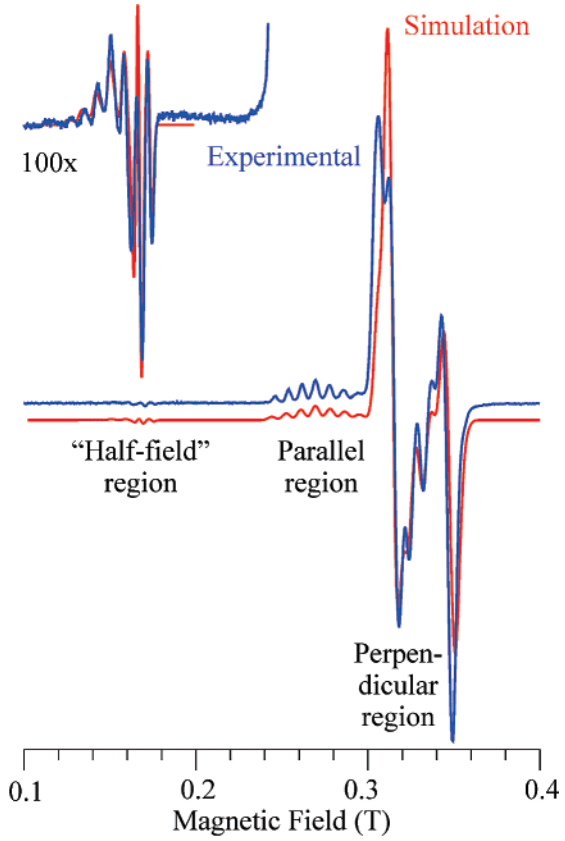

Figure 6. Experimental (blue traces) and simulated (red traces) X-band EPR spectra of **5**. Experimental conditions: $T = 30$ K; microwave frequency = 9.475 GHz; microwave power = 0.201 mW; 100 kHz field modulation amplitude, 2.5 mT (10 G = 1 mT); time constant = 10.24 ms; scan time = 20.97 s. Simulation parameters: coupled two-spin system with $S_1 = S_2 = {}^1/_2$; isotropic exchange coupling, $J = -100$ cm^{-1} (JS_1S_2); dipolar coupling, $D = 0.065$ cm^{-1}. Parameters for each spin: $\mathbf{g}_{S_1} = \mathbf{g}_{S_2} = [2.055, 2.070, 2.274]$; $\mathbf{A}(^{63}Cu_{S1}) = \mathbf{A}(^{63}Cu_{S2}) = [50, 50, 520]$ MHz. Gaussian single-crystal line widths (hwhm) = 80 MHz. The different regions of the spectrum are indicated and the inset shows a 100× expansion of the "half-field" region.

suggesting that the phenolate group is not involved in redox processes under these experimental conditions. Thus, the redox behavior of $[Cu^{II}_2(PD'O^-)(H_2O)_2]^{3+}$ (**5**) is due to the coupled dinuclear copper centers. EPR data described below further support the formulation of a wholly Cu-centered paramagnetic system.

EPR Spectroscopy. The X-band EPR spectrum of mononuclear copper(II) complex $[Cu^{II}(mPD'OH)(H_2O)]^{2+}$ (**6**) at 34 K is presented in the Supporting Information (Figure S6) together with a simulation. The spectrum is typical for Cu(II) in a tetragonally distorted environment, with the following spin Hamiltonian parameters: $g_x = 2.055$, $g_y = 2.070$, $g_z = 2.274$ (defined as $g_z \equiv g_{max} \equiv g_{||}$, $g_y \equiv g_{mid}$, $g_x \equiv g_{min}$), $A_{x,y}$ ($A_\perp$) = 50 MHz (estimated), A_z ($A_{||}$) = 530 MHz. These values for $A_{||}$ and $g_{||}$ are exactly within the range described by Peisach and Blumberg[48] for Cu(II) with an equatorial N_3O_1 donor set and an overall charge of 2+. The electronic structure of the Cu(II) ion in **6** is thus quite usual.

In contrast, the EPR spectrum of dinuclear complex $[Cu^{II}_2(PD'O^-)(H_2O)_2]^{3+}$ (**5**) recorded at 30 K and its simulation are quite remarkable (Figure 6). Qualitatively, the

(43) Belle, C.; Beguin, C.; Gautier-Luneau, I.; Hamman, S.; Philouze, C.; Pierre, J. L.; Thomas, F.; Torelli, S. *Inorg. Chem.* **2002**, *41*, 479−491.
(44) Torelli, S.; Belle, C.; Gautier-Luneau, I.; Pierre, J. L.; Saint-Aman, E.; Latour, J. M.; Le Pape, L.; Luneau, D. *Inorg. Chem.* **2000**, *39*, 3526−3536.
(45) Michel, F.; Torelli, S.; Thomas, F.; Duboc, C.; Philouze, C.; Belle, C.; Hamman, S.; Saint-Aman, E.; Pierre, J. L. *Angew Chem. Int. Ed.* **2005**, *44*, 438−441.
(46) Torelli, S.; Belle, C.; Hamman, S.; Pierre, J. L.; Saint-Aman, E. *Inorg. Chem.* **2002**, *41*, 3983−3989.
(47) Koval, I. A.; Huisman, M.; Stassen, A. F.; Gamez, P.; Roubeau, O.; Belle, C.; Pierre, J. L.; Saint-Aman, E.; Luken, M.; Krebs, B.; Lutz, M.; Spek, A. L.; Reedijk, J. *Eur. J. Inorg. Chem.* **2004**, 4036−4045.
(48) Blumberg, W. E.; Peisach, J. *Arch. Biochem. Biophys.* **1974**, *162*, 502−512.

spectrum exhibits a doubling of the perpendicular region and a multiline pattern in the parallel region. Additionally, there is a weak but well-resolved multiline pattern at the "half-field" position (~0.16 T, effective $g \approx 4.2$).

As explained more than fifty years ago by Bleaney and co-workers[27] for the case of copper(II) acetate, such an EPR spectrum results from magnetic exchange coupling between two electronic spins, here both Cu(II) $S = 1/2$ as in $Cu_2(OAc)_4$, to give a coupled effective spin triplet, $S_{tot} = 1$. In the case of $Cu_2(OAc)_4$, the coupling is antiferromagnetic ($J > 0$ using the JS_1S_2 formalism) because of a direct orbital overlap pathway. There is also a pseudo metal−metal bond so that the ground-state manifold is $M_{Stot} = 0$ and the EPR spectra are visible only at higher temperatures. In the case of **5**, EPR spectra are visible at low temperatures (<100 K), indicating that coupling must be ferromagnetic ($J < 0$ using the JS_1S_2 formalism) and the ground-state manifold is $M_{Stot} = \pm 1$ (in zero field). The magnitude of the isotropic exchange coupling is not known and not significant for our purposes here. Observing the strong coupling (i.e., greater than the Zeeman splitting and hyperfine and dipolar couplings) is sufficient. Accordingly, for the EPR simulations, we arbitrarily set $J = 100$ cm^{-1} (JS_1S_2 formalism). The splitting in the perpendicular region allows an estimate for the magnitude of the dipolar coupling, D. Use of single-ion spin Hamiltonian parameters identical to those determined for mononuclear complex **6** and refinement of the dipolar coupling allowed a very good fit to the observed spectrum (Figure 6).[49]

The simulation also reproduces the intensity and splitting pattern of the half-field multiline signal (Figure 6, inset). The observed hyperfine splitting in the half-field feature (as well as in the parallel feature) in the EPR spectrum of **5** is half the magnitude observed for **6** (~80 vs ~160 G, respectively) and exactly as expected for a spin-coupled $S_1 = S_2 = 1/2$ system on the basis of spin vector (Clebsch−Gordan) coupling coefficients.[27] This correspondence is strong evidence that the EPR spectrum of **5** can best be represented as the result of ferromagnetic coupling between two mononuclear analogues such as **6**. Last, the dipolar coupling determined by simulation, $D = 0.065(5)$ cm^{-1}, can be related to the distance between the two Cu(II) ions in **5**

(49) The fit is not perfect; there are many reasons for this, which we will briefly enumerate. Complexes **5** and **6** do not have identical coordination geometry about the Cu(II) ion(s). As described above, the Cu(II) ions in the former are in a more ideal square pyramidal geometry and the phenol ligand is protonated in the latter. Such geometrical and electronic differences could affect the spin Hamiltonian parameters for Cu(II). However, to make the problem tractable, we had to assume that there were no changes in single ion parameters (g values, hyperfine couplings, and line widths) between the single Cu(II) ion in **6** and each Cu(II) site in **5**. Ideally, a mixed CuZn complex of PD′O$^-$ might provide the desired information, but given that the Zn geometry in **7** is different from that of Cu in **5**, such a putative complex could well be a less-than-ideal model for single ion sites in **5**. We also assume that the two sites in **5** are electronically identical, which is likely, but is not imposed by crystallographic symmetry. Equally important, for simplicity, we assume that the dipolar coupling between the two Cu(II) ions in **5** is strictly axial (i.e., $E = 0$) and that the single-ion electronic coordinate systems of the two are collinear. Despite these caveats, the simulation of the X-band EPR spectrum of **5** is successful and yields a dipolar coupling of $D = 0.065(5)$ cm^{-1} (Figure 6).

Chart 5

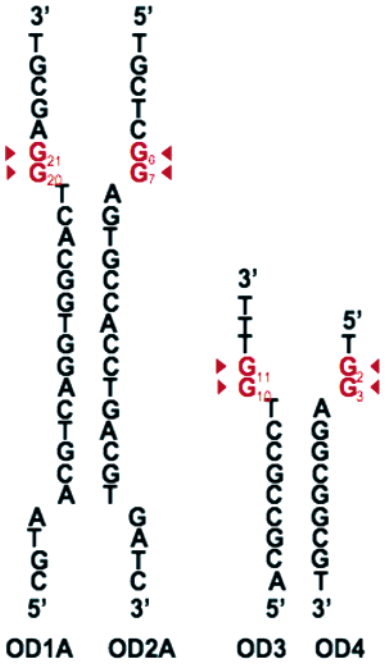

by use of equations developed by Snetsinger et al.[50] With a crystallographic Cu−Cu distance of 4.126 Å, these equations yield a maximum coupling of ~0.055(5) cm^{-1}, which is reasonably close to the experimental coupling of 0.065(5) cm^{-1} considering the very simplified collinear, purely through-space dipolar coupling nature of the calculation.

A frozen solution EPR spectrum of the guanosine-containing complex $[Cu^{II}_2(PD'O^-)(G)]^{3+}$ (**8**) (see the Supporting Information, Figure S7)[29] is very similar (although with less resolution) to the distinctive spectrum of $[Cu^{II}_2(PD'O^-)(H_2O)_2](ClO_4)_3$ (**5**) (Figure 6). Both exhibit a seven-line half-field region signal with $g \approx 4.2$. This, in addition to the X-ray structural analysis (Figure 4A), indicates that **8** retains its dinuclear structure in solution, including a Cu−Cu juxtaposition and Cu···Cu distance similar to those of **5** (Figure 1).

(2) Identification of Guanine as the Target of DNA Oxidation. Selective Guanine Oxidation Induced by $[Cu^{II}_2(PD'O^-)(H_2O)_2](ClO_4)_3\cdot 3H_2O$ (5). Selective oxidation of guanine residues by $[Cu^{II}_2(PD'O^-)(H_2O)_2](ClO_4)_3\cdot 3H_2O$ (**5**) was discovered by surveying its reactivity with the oligodeoxynucleotide system of OD1A/OD2A (Chart 5). This DNA contains a single- and double-stranded junction in which the first and second unpaired positions (n and $n + 1$) are both occupied by guanines. Little direct strand scission was observed after incubating OD1A/OD2A with 100 μM **5** and 5 mM MPA (MPA = 3-mercaptopropionic acid) for 15 min at ambient temperature (Figure 7, lane 4). However, subsequent treatment of this mixture with hot piperidine induced scission primarily at the Gs in the junction, a result of their selective oxidation (Figure 7, lane 4′). No equivalent reaction is evident in the absence of any one component of the mixture, OD1A, OD2A, **5**, or MPA (Figure 7). Equivalent

(50) Snetsinger, P. A.; Chasteen, N. D.; van Willigen, H. *J. Am. Chem. Soc.* **1990**, *112*, 8155−8160.

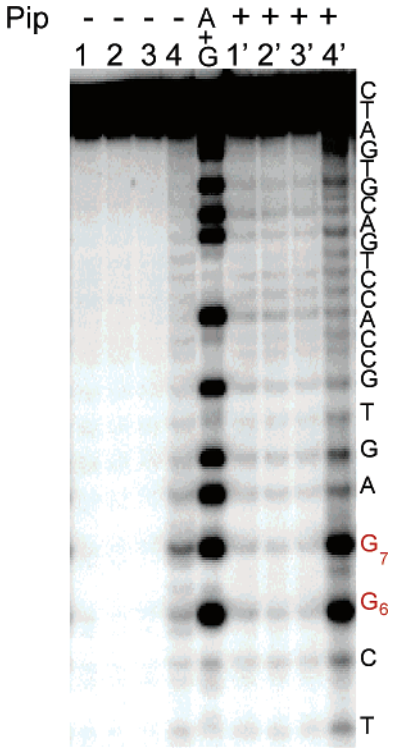

Figure 7. Autoradiogram of a 20% polyacrylamide denaturing gel (7 M urea) of products formed by incubation (15 min) of 100 nM 5′-^{32}P-labeled OD2A in the presence of OD1A, **5**, and MPA in sodium phosphate at ambient temperature (10 mM, pH 6.8) without (lanes 1−4) and with (lanes 1′−4′) subsequent piperidine (Pip) treatment. Lanes 1 and 1′, OD2A alone; lanes 2 and 2′, OD1A/OD2A with 5 mM MPA; lanes 3 and 3′, OD1A/OD2A with 100 μM **5**; lanes 4 and 4′, 100 μM **5** with 5 mM MPA and OD1A/OD2A.

data had previously been observed for the Gs of OD1A in the junction.[25]

ESI-MS Analysis of Guanine Oxidation Products. Because piperidine-induced strand cleavage may result from many products, mass spectrometry was used to characterize the DNA products formed by **5** in detail. This approach benefits from use of a minimal molecular weight of DNA; thus, a new oligodeoxynucleotide pair (OD3/OD4) (Chart 5) was selected. This target retained the Gs at the junction and exhibits the same reaction pattern as OD1A/OD2A with $[Cu^{II}_2(PD'O^-)(H_2O)_2](ClO_4)_3{\cdot}3H_2O$ (**5**)/MPA/O_2.[25] Reaction of OD3/OD4 was also extended for 2 h to increase the yield of oxidation products. The oligodeoxynucleotide products were isolated by reverse-phase HPLC, desalted, and analyzed by ESI-MS. Two major species were detected for each strand (OD3 and OD4). One species revealed a mass gain of +18 amu over the parent compound whereas the other exhibited a mass gain of +34 amu by comparison to the parent strand (Figure 8). Several minor products were also detected (see Figure 8B and the Supporting Information, Table S7). The +18 amu mass gain is consistent with the formation of 2,6-diamino-5-formamidino-4-hydroxy-pyrimidine (FAPy-G, Chart 6). Little precedence is available for the species with a mass gain of +34 amu, but Meunier and co-workers proposed this to be 5,8-dihydroxy-7,8-dihydroguanine (5,8-di-OH-G, Chart 6).[51] However, this derivative is likely to be hydrolytically

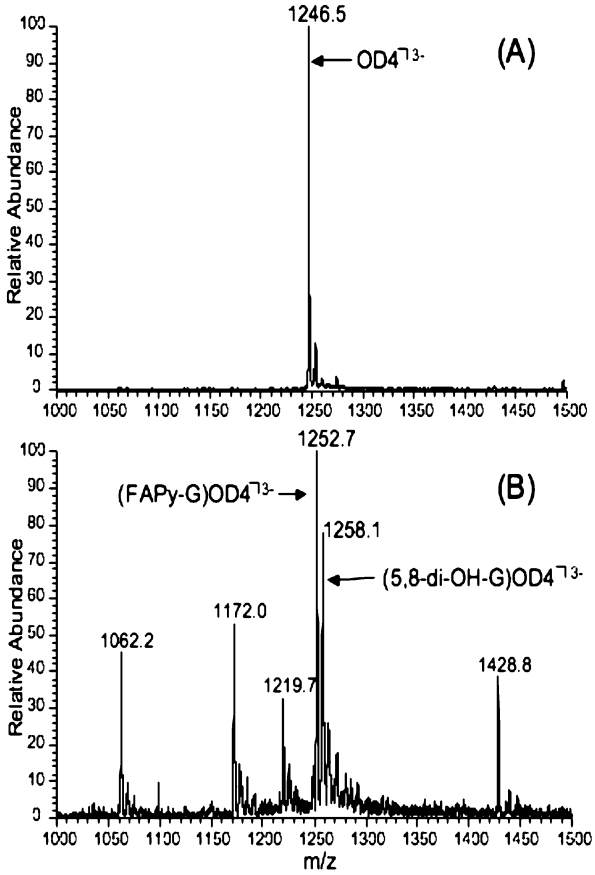

Figure 8. ESI/MS analysis of OD4 incubation (aerobic, 2 h) with **5** and MPA in the presence of OD3 at ambient temperature. ESI/MS spectra of material eluting from the HPLC (A) between 25.8 and 27 min (OD4) and (B) between 22.1 and 23.5 min for isolation of the two major oxidation products. Only 3− charged mass spectrometric signals are shown. The calculated (instrument deconvolution program) molecular weights are 3742.2 (= 3·[1246.5 + H^+]) for OD4 in (A), 3759.8 for (FAPy-G)OD4 (+18 amu), and 3777.5 for (5,8-di-OH-G)OD4 (+34 amu).

Chart 6

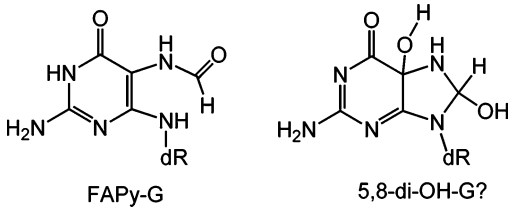

unstable and may undergo a rearrangement to yield a more stable isomer.

Guanine Oxidation by Mononuclear Complex 6. Selective and efficient oxidation of DNA by multinuclear copper complexes had not previously been supported under equivalent conditions by their mononuclear analogues,[21,22] and the generality of this observation now extends as well to $[Cu^{II}(mPD'OH)(H_2O)]^{2+}$ (**6**) (Chart 2), the mononuclear analogue of **5**. Complex **6** promoted only background oxidation of OD1A/OD2A without regard to sequence or structure and still required a secondary treatment of piperidine to detect any strand fragmentation (see the Supporting Information, Figure S9).[29] Such a result is likely caused by diffusible

(51) Vialas, C.; Claparols, C.; Pratviel, G.; Meunier, B. *J. Am. Chem. Soc.* **2000**, *122*, 2157−2167.

radicals generated by **6** in the presence of MPA and O_2. If the radical remains associated with the copper, the mononuclear complex lacked the ability to bind DNA selectively and direct its oxidant to a specific site. A comparable nonspecific background level of reaction is also generated with **5** concurrently with its targeted reaction at a ss/ds junction. All multinuclear copper complexes that support selective oxidation of DNA to date similarly induce a low level of nonspecific reaction as well.[21−23,29]

(3) Sequence and Conformation Dependence of Guanine Oxidation. Dependence on Guanine at the Junction of Single- and Double-Stranded DNA. Both di- and trinuclear copper complexes **1** and **2** described previously demonstrated specific requirements for purines in general, and guanine most commonly, to support selective reaction of DNA at junctions of single- and double-stranded (ss/ds) DNA.[21−24] The presence of four unpaired Gs extending from the duplex formed by OD1A/OD2A offered an optimum target to begin characterizing $[Cu^{II}_2(PD'O^-)(H_2O)_2](ClO_4)_3$ (**5**) and the significance of each G became apparent after their successive replacement by A or C. Under standard conditions, **5** consumed approximately 1% of OD1A and 5% of OD2A after 15 min in the presence of MPA and O_2. Substituting A for G at position *n* of OD2A, the first unpaired site on the 5′-extension, reduced the overall consumption of OD1A and OD2B to 0.6 and 3.6%, respectively, under equivalent conditions (see the Supporting Information, Figures S10 and S11).[29] Further substitution of G resulted in an additional decrease in consumption of the DNA to a basal level of 0.5%. This level represents the nonspecific background oxidation distributed throughout the oligodeoxynucleotide and common to the mono-, di-, and trinuclear copper complexes. This loss of site-selective reaction is also reflected in the relative yield of oxidation at each site within the ss/ds junction. First, the site-selective reaction remained specific for G, and replacement of G by an A or C resulted in a decreased yield of scission to background levels at the sites of substitution. Second, the Gs surrounding the sites of the substitution reaction were oxidized less efficiently. For example, the relative yield of oxidization diminished by ∼37% at the two unpaired Gs in OD1A across from a 5′-GA extension in OD2B (Figure 9B). An alternative substitution of a 5′-AG extension in OD2C diminished reaction of the G in this extension and supported the same diminished yield of reaction of OD1A as that with the original 5′-GA extension. (Figure 9C). Substitution of both Gs extending from the duplex region of OD2A or complete loss of this extension suppressed reaction of the Gs in OD1A extending from the duplex to almost-background levels (D and E of Figure 9).

Dependence on a Junction between Single- and Double-Stranded DNA. The role of the DNA junction in directing selective reaction was examined with a series of oligodeoxynucleotide pairs that maintained the optimum four Gs at an increasing distance from the duplex region (Figure 10). Insertion of a single pair of pyrimidines between the duplex and the four extrahelical Gs decreased the selective oxidation of G by a little less than 25% under standard conditions with

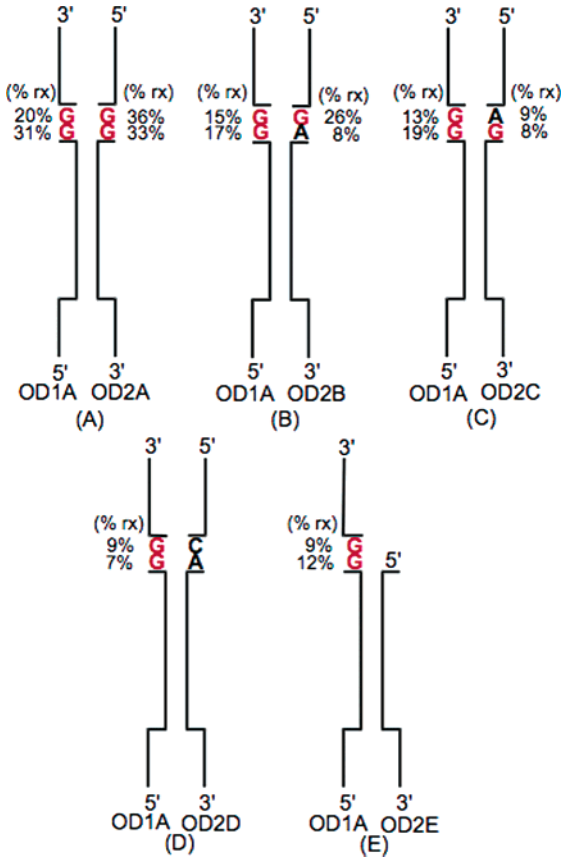

Figure 9. Relative selectivity for oxidation promoted by **5** at the indicated sites (see the Supporting Information, Figures S10 and S11).

5 (A vs B in Figure 10). Additional intervening Ts further reduced the yield of selective oxidation (C and D of Figure 10). However, preferential reaction at the unpaired Gs was not completely eliminated by the presence of three intervening Ts (Figure 10D). The overall consumption of the oligodeoxynucleotides decreased only from 1.4 to 1.1% for OD1A to OD1H and 6.7 to 1.8% for OD2A to OD2H.

Preferential reaction of Gs in the ss/ds junction suggested that the reactive assembly with **5** requires some structural constraints because the G cluster at a distance from the junction or in single-stranded DNA[25] is a weak target of reaction. A cluster of four Gs was also embedded within a duplex by annealing OD1A with OD5 in order to test the effect of the most restrictive environment (Figure 11). This pair of oligodeoxynucleotides allowed for direct comparison between oxidation of Gs in a ss/ds junction and those surrounded by duplex structures. No oxidation of G above background was detected under standard conditions with **5** for the Gs held by adjacent duplex regions, whereas the Gs of the ss/ds junction reacted quite prominently and with efficiencies equivalent to those measured for the OD1A/OD2A pair (Figures 11 and the Supporting Information, Figure S14).[29]

(4) Reactants Required for Guanine Oxidation. Dependence on MPA. Thiols in general and MPA in particular are typically used to reduce copper(II) to their copper(I) derivatives in situ.[1−3] The copper(I) intermediates then combine with ambient concentrations of O_2 to form the

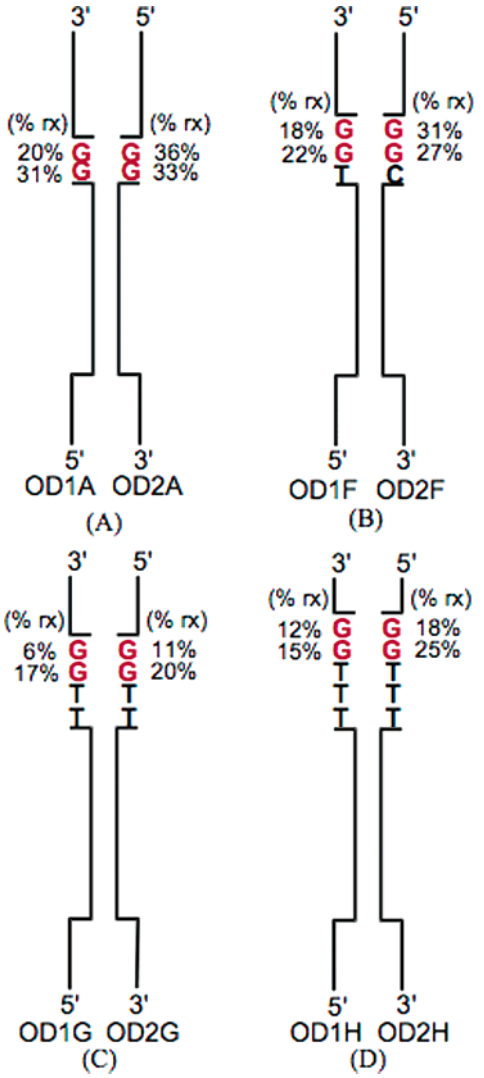

Figure 10. Relative reactivity of Gs progressively moved farther from the duplex region in the presence of complex **5**, MPA, and O_2 (see the Supporting Information, Figures S12 and S13).

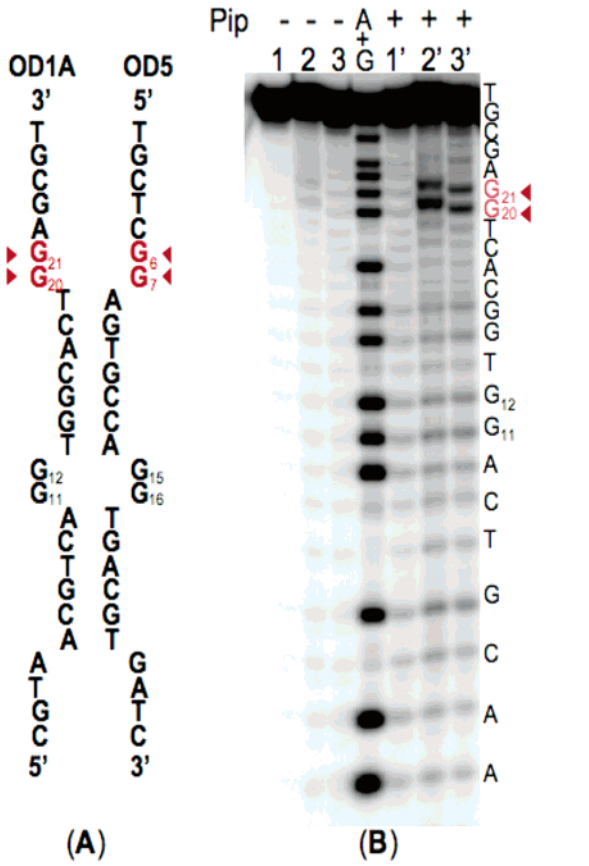

Figure 11. Autoradiogram of a 20% polyacrylamide denaturing gel (7 M urea) showing strand scission of 100 nM 5′-^{32}P-labeled OD1A in the alternative presence of OD2A and OD5 after standard aerobic incubation with **5** and MPA for 15 min. Lane 1, 1′, OD1A without reactants; lane 2, 2′, OD1A/OD2A; Lane 3, 3′, OD1A/OD5; Lanes 1′−3′ were treated with 0.2 M piperidine treatment (Pip) at 90 °C for 30 min after isolation from the reaction mixture.

ultimate oxidant used to react with DNA. To explore the possible influence of MPA in guanine oxidation promoted by **5**, we also used two alternative thiols, β-mercaptoethanol (ME) and dithiothreitol (DTT), as well as ascorbate as reductants to initiate reaction. Neither ME nor DTT supported reaction of the di- and trinuclear copper complexes **1** and **2** as efficiently as MPA in previous studies.[21,22] In contrast, ascorbate dramatically accelerated reaction of these complex.[21,22] The enhanced activity promoted by ascorbate is likely due to its lack of binding (versus thiol) to the multinuclear complexes in competition with the DNA target. Surprisingly, guanine oxidation by **5** was completely suppressed when ME, DTT, or ascorbic acid was used instead of MPA under otherwise standard reaction conditions (see the Supporting Information, Figure S15). Guanine oxidation was similarly not detected when the standard concentration of MPA (5 mM) was supplemented with 2.5 mM DTT (see the Supporting Information, Figure S16). Either MPA plays a unique role in the activation of **5** or its chemical and physical properties provide an essential balance needed to reduce the Cu^{II}_2, but not the $Cu^{II}_2O_2$ derivative of **5**.

Dependence on O_2. A requirement of O_2 for oxidation of DNA by a range of copper complexes including the multinuclear complexes **1** and **2** has already been confirmed.[21,22,52,53] To test this requirement for **5**, we repeated the reaction of OD1A/OD2A under an O_2-limited environment. These conditions suppressed the overall reaction of OD1 by 90% and reduced the selective oxidation of Gs at the ss/ds junction to nearly background levels (Figure 12 and the Supporting Information, Figure S17).[29] Thus, **5** appears to combine with O_2 to generate an oxidant capable of selective reaction with G.

Sensitivity of Guanine Oxidation to Radical Scavengers. The selectivity of DNA oxidation by **5** is most consistent with generation of reactive intermediates that are not highly diffusible. The ultimate oxidant of DNA generated by **5** was also found to be insensitive to competitive hydrogen-atom donors. The presence of 10 mM ethanol, D-mannitol, or *tert*-butyl alcohol led to scavenging of radicals such as $^{\bullet}$OH, but this treatment did not significantly effect consumption of OD1A/OD2A (Figure 12 and the Supporting Information, Figure S17).[29] This insensitivity to radical traps is consistent

(52) Sigman, D. S.; Mazumder, A.; Perrin, D. M. *Chem. Rev.* **1993**, *93*, 2295−2316.
(53) Pogozelski, W. K.; Tullius, T. D. *Chem. Rev.* **1998**, *98*, 1089−1107.

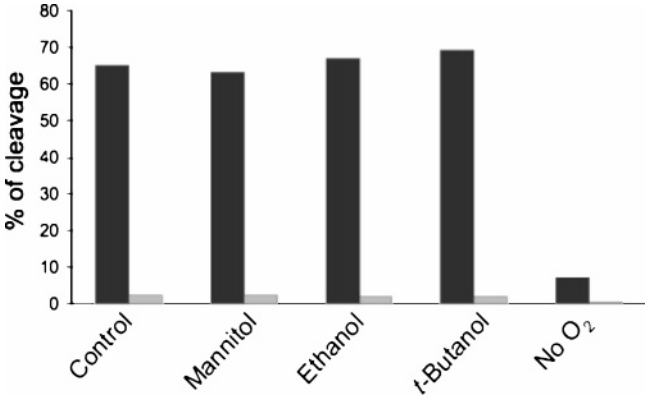

Figure 12. Effect of radical scavengers and limiting O_2 on strand scission of ^{32}P-OD1A/OD2A promoted by complex $[Cu^{II}_2(PD'O^-)(H_2O)_2]^{3+}$ (**5**) under standard conditions in the absence and presence of radical scavengers (10 mM) (see the Supporting Information, Figure S17, for experimental details). Overall consumption of OD1 is indicated by the light gray shading and the percentage of specific strand scission at $G_{22} + G_{21}$ by the dark shading.

with results of the other multinuclear copper complexes and suggests the formation of copper-bound oxidant.[21,22,52,53]

Discussion

Coordination Chemistry of $[Cu^{II}_2(PD'O^-)(H_2O)_2]^{3+}$ (5). The X-ray structure of $[Cu^{II}_2(PD'O^-)(H_2O)_2]^{3+}$ (**5**) shows that the two copper ions are closely linked via a phenolate oxygen bridging atom. Electrochemical and EPR spectroscopic studies also reveal close electronic communication. Crosstalk between copper(II) centers in **5** is indicated by the observation that reduction of one copper ion (Cu^{II}/Cu^{I} process) is followed by reduction of the second center but at a different (by 0.29 V) potential. This characteristic is not exhibited by non-phenolate-bridged complexes, for example, $[Cu^{II}_2(D^1)(H_2O)_2]^{4+}$ (**1**) (Chart 1), for which only one peak (Cu^{II}/Cu^{I} process) is observed.[54] In this latter example, the two copper ion sites act independently. The EPR spectroscopic analysis of $[Cu^{II}_2(PD'O^-)(H_2O)_2]^{3+}$ (**5**) also highlights a coupling of the two copper ions through the phenolate oxygen bridge. The distinctive half-field line with seven-line pattern (each copper ion with $I = 3/2$) leads to the conclusion that the copper(II) ions are ferromagnetically coupled ($S = 1$, ground state) through the phenolate oxygen.

The synthesis and X-ray structural determinations of guanosine (G) adducts with dicopper(II) and dizinc(II) complexes of $PD'O^-$, $[Cu^{II}_2(PD'O^-)(G)]^{3+}$ (**8**), and $[Zn^{II}_2(PD'O^-)(G)]^{3+}$ (**9**) also provide insight into the reaction of **5** with DNA. An EPR spectrum of **8** (see the Supporting Information) reveals a coordination and electronic structure very similar to that of $[Cu^{II}_2(PD'O^-)(H_2O)_2]^{3+}$ (**5**), i.e., with ferromagnetically coupled copper ions. More importantly, the structures of **8** and **9** reveal that the dicopper−$PD'O^-$ framework can readily bind and bridge a guanine moiety. Taken together, these structures and the known O_2 chemistry of the reduced form of **5**,[55] $[Cu^{I}_2(PD'OH)(RCN)_2]^{2+}$, provide a rational explanation for selective reaction of DNA and suggest likely intermediates involved in the reaction of **5**.

Target Recognition by $[Cu^{II}_2(PD'O^-)(H_2O)_2](ClO_4)_3$ (5). The similarity of DNA sites oxidized by multinuclear copper complexes **1**, **2**, and **5** suggest a common mode of recognition. All of these complexes act preferentially at junctions of single and double strands (ss/ds) of DNA. Efficient reaction is not observed for ss or ds DNA alone.[21−23,25,56] The myriad of conformations available to ss DNA may effectively compete against its productive association with the metal complex, and duplex DNA may not accommodate the conformation required for localizing and orienting this complex. A ss/ds junction may uniquely offer the proximity of two DNA strands and yet retain sufficient flexibility to assemble with the copper complex for reaction. Such interactions do not appear to compete with Watson−Crick base pairing, because potential target sequences within duplex DNA remain protected from reaction. The limited flexibility of a GG/GG mismatch surrounded by a duplex formed by OD1A/OD5 was also not sufficient for recognition by **5** (Figure 11). Furthermore, this mismatch region did not act as an entry for unwinding DNA in the presence of the multinuclear copper complex, because the potential ss/ds junction was not susceptible to oxidation.

The efficiency of DNA oxidation is also sensitive to incremental changes in the flexibility of target sequences. This result is most clearly demonstrated with **5** by the decrease in the oxidation of GG sequences that are not directly adjacent to a duplex (OD1G/OD2G vs OD1A/OD2A) (Figure 10). The trinuclear copper **2** (Chart 1) had previously exhibited a similar sensitivity to the restrictions placed on a ss/ds junction. In this case, reaction was suppressed as the flexibility of the single-stranded extensions from a ss/ds junction was decreased by joining their termini to form a loop of 11 residues.[24]

Each multinuclear complex investigated to date has shown a unique dependence on nucleotide sequence surrounding its target junction, but all are related by a requirement for multiple purines in general and guanines most often.[21−23,25,56] This type of dependence is typically indicative of metal−purine coordination. G N7 is a strong ligand for transition metals such as copper[57,58] and has the potential to control association and orientation of a metal oxidant. Replacing a single G with 7-deazaguanine in a reactive ss/ds junction of DNA severely inhibited target oxidation by **2** even though multiple Gs are necessary for efficient reaction.[24] This result provided the first direct evidence that the multinuclear copper complexes are indeed guided by their interaction with guanine. However, a single guanine alone is still not adequate for directing reaction of **5** (Figure 9) or, as described

(54) Lee, D. H.; Wei, N.; Murthy, N. N.; Tyeklar, Z.; Karlin, K. D.; Kaderli, S.; Jung, B.; Zuberbuhler, A. D. *J. Am. Chem. Soc.* **1995**, *117*, 12498−12513.

(55) Li, L.; Sarjeant, A. A. N.; Vance, M. A.; Zakharov, L. N.; Rheingold, A. L.; Solomon, E. I.; Karlin, K. D. *J. Am. Chem. Soc.* **2005**, *127*, 15360−15361.

(56) Humphreys, K. J.; Johnson, A. E.; Karlin, K. D.; Rokita, S. E. *J. Biol. Inorg. Chem.* **2002**, *7*, 835−842.

(57) Sabat, M.; Lippert, B. *Met. Ions Biol. Syst.* **1996**, *33*, 143−176.

(58) DeRose, V. J.; Burns, S.; Vogt, M.; Kim, N.-K. In *Comprehensive Coordination Chemistry II*; McCleverty, J. A., Meyers, T. J., Eds.; Elsevier: Oxford, 2003; pp 787−813.

previously, **1** and **2**.[21−23,56] A cluster of four guanines appears optimal for **5**. This may reflect the ability of the dicopper complex to coordinate two proximal Gs. The crystal structures of $[Cu^{II}_2(PD'O^-)(G)]^{3+}$ (**8**) and $[Zn^{II}_2(PD'O^-)(G)]^{3+}$ (**9**) demonstrate the ability of the metals to act cooperatively in coordination to a single G, and a similarly cooperativity can be expected for the N7 positions of neighboring Gs. Related dimetal coordination of guanine has previously been detected in complexes of Rh, Ru, Mo, and Zn.[59−61]

Target Oxidation by $[Cu^{II}_2(PD'O^-)(H_2O)_2](ClO_4)_3$ (5). The multinuclear copper complexes exhibit remarkably different oxidative chemistry with DNA despite their similarities in target recognition. Both complexes **1** and **2** promote direct strand scission of DNA that is consistent with hydrogen-atom abstraction at the phosphoribose backbone.[21−23,56] The efficiency of this reaction is also very high. For example, 14% of a target strand at 1 μM is consumed over 15 min in the presence of as little as 1 μM **1** and excess MPA.[21] Under these conditions, 79% of the oxidation occurs at the single nucleotide that is targeted for oxidation by this complex. No reaction is observed under equivalent conditions when OD1A/OD2A is incubated in the presence of a 20-fold greater concentration of **5** (see the Supporting Information, Figure S8).[29] Even after increasing the concentration of **5** to 100 μM, only between 2 and 7% of its target strands are consumed (Figure 7).[29]

More importantly, oxidation of DNA by complex **5** in the presence of MPA and O_2 does not promote spontaneous strand scission (Figure 7). Instead, fragmentation of the DNA is observed only after treatment with piperidine after oxidation by **5**. The sites of fragmentation indicate that reaction localizes to the Gs within the ss/ds junction, but this assay does not provide conclusive evidence on the exact nature of the oxidation product(s), because a variety of derivatives are sensitive to piperidine treatment.[19] The nucleobase guanine is most easily oxidized, and its products often exhibit lability under piperidine treatment; however, oxidation of the C1′ position of deoxyribose to form the ribonolactone also exhibits a similar lability.[19] Unambiguous identification of the DNA products generated by **5** was achieved by ESI-MS. Both chemical characterization[25] and MS identified FAPy-G as the major product of the reaction (Figure 8). A minor product with a mass 34 amu greater than that of the parent strand was also detected, but no trace of the most common product of G oxidation, 8-oxoguanine, was discovered.

One mechanism by which FAPy-G has been previously suggested to form involves the initial addition of a hydroxyl radical to G followed by a second addition of a hydrogen atom (or $1e/1H^+$).[62−65] The initial radical reaction generates an intermediate common to both 8-oxoguanine and FAPy-G

Scheme 2

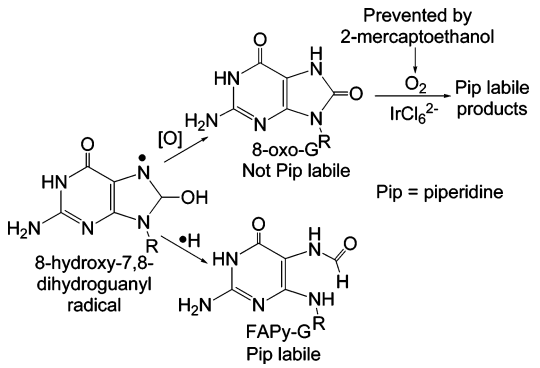

production (Scheme 2). Partitioning to FAPy-G is dominant for **5** most likely because of the presence of excess thiol used to reduce the dicopper(II) moiety within $[Cu^{II}_2(PD'O^-)(H_2O)_2](ClO_4)_3$ (**5**) to a dicopper(I) species that in turn initiates the activation of O_2. These processes provide a direct contrast to the reactions promoted by free Cu^{II} salts and H_2O_2 that appear to generate 8-oxoguanine through a mechanism involving singlet oxygen.[66,67]

Reaction between DNA and **5** is surprisingly sensitive to the choice of added thiol. Only MPA supports target-selective modification of DNA, and neither ME nor DTT are effective substitutes (see the Supporting Information, Figure S16).[29] Whereas the strong reducing potential of DTT (−0.33V vs NHE)[68] may quench the reactive $Cu^{II}_2O_2$ intermediate generated by **5**, a similar proposal for ME could not be made on the basis of the redox potential. ME and MPA share similar potentials (−0.196 and −0.20 V vs NHE, respectively).[69,70] The ability of MPA to quench intermediates of **5** formed on the surface of DNA may be limited by electrostatic repulsion between the anionic MPA and DNA. However, equivalent repulsion would also be expected to hinder reduction of the parent dicopper(II) complex on DNA as well.[71] The role of thiol is undoubtedly complex because of its multiple functions and strong ability to coordinate copper in competition with DNA and O_2. A more limited dependence on thiol structure had previously been observed for reaction of complexes **1** and **2**,[21,22] but nonspecific background oxidation of DNA in the alternative presence of **1**, **2**, or **5** is not very sensitive to the choice of thiol (Figure S16).

Formation of a Cu_2-O_2 Intermediate for DNA Oxidation. Multinuclear copper complexes significantly lower the entropic barrier and reduce the time scale for activation of

(59) Zamora, F.; Sabat, M. *Inorg. Chem.* **2002**, *41*, 4976−4977.
(60) Crawford, C. A.; Day, E. F.; Saharan, V. P.; Folting, K.; Huffman, J. C.; Dunbar, K. R.; Christou, G. *Chem. Commun.* **1996**, 1113−1114.
(61) Dunbar, K. R.; Matonic, J. H.; Saharan, V. P.; Crawford, C. A.; Christou, G. *J. Am. Chem. Soc.* **1994**, *116*, 2201−2202.
(62) (a) Neeley, W. L.; Essigmann, J. M. *Chem. Res. Toxicol.* **2006**, *19*, 491−505. (b) Pratviel, G.; Meunier, B. *Chem.−Eur. J.* **2006**, *12*, 6018−6030.
(63) Cadet, J.; Delatour, T.; Douki, T.; Gasparutto, D.; Pouget, J. P.; Ravanat, J. L.; Sauvaigo, S. *Mutat. Res.* **1999**, *424*, 9−21.
(64) Cadet, J.; Berger, M.; Douki, T.; Ravanat, J. L. *Rev. Physiol. Biochem. Pharmacol.* **1997**, *131*, 1−87.
(65) Cadet, J.; Douki, T.; Frelon, S.; Sauvaigo, S.; Pouget, J. P.; Ravanat, J. L. *Free Radical Biol. Med.* **2002**, *33*, 441−449.
(66) Yamamoto, K.; Kawanishi, S. *J. Biol. Chem.* **1989**, *264*, 15435−15440.
(67) Frelon, S.; Douki, T.; Favier, A.; Cadet, J. *Chem. Res. Toxicol.* **2003**, *16*, 191−197.
(68) Cleland, W. W. *Biochemistry* **1964**, *3*, 480.
(69) Keire, D. A.; Strauss, E.; Guo, W.; Noszal, B.; Rabenstein, D. L. *J. Org. Chem.* **1992**, *57*, 123−127.
(70) Millis, K. K.; Weaver, K. H.; Rabenstein, D. L. *J. Org. Chem.* **1993**, *58*, 4144−4146.
(71) Thederahn, T. B.; Kuwabara, M. D.; Larsen, T. A.; Sigman, D. S. *J. Am. Chem. Soc.* **1989**, *111*, 4941−4946.

O_2 through the formation of Cu_2O_2 intermediates (i.e., peroxide and hydroperoxide derivatives) relative to their equivalent formation with mononuclear complexes.[72] The significance of this effect is illustrated by the consistent lack of DNA modification when the multinuclear complexes **1**, **2**, and now **5** are replaced by their mononuclear derivatives (for example, complex **6**, see the Supporting Information, Figure S9).[21,22] Ligand chemistry and geometry also dramatically affect the nature of the Cu_2O_2 intermediate.[20,73,74] As a predictive understanding of these variables develops, metal complexes may be designed to modify specific functional groups, conformations, or nucleotide sequences of DNA on demand.[18]

The versatility of copper complexes is evident by comparing the reaction of DNA supported by complexes **1** and **2** vs complex **5**. Differences in the reaction efficiency of complexes **1** and **2** vs **5** may result from variation in either of their affinities for DNA targets or in the chemistry of their $Cu^{II}_2O_2$ intermediates. In contrast, differences in the products formed by these complexes likely reflects only the varying chemistry of the intermediates. An alternative explanation on the basis of restricted orientation of the ultimate oxidant to favor either nucleobase or phosphoribose backbone reaction is unlikely, because the targeted junctions are expected to be dynamic and adopt a range of conformations.

Model studies on the copper(I) forms of both **1** and **5** reveal significant differences in their intermediates formed after the addition of O_2. In organic solvents at −80 °C, the copper(I) form of **1** reacts with O_2 to yield an end-on Cu−O−O−Cu peroxide dicopper(II) species.[54,55,75] An additional series of dicopper complexes has been found to generate a side-on peroxo-dicopper(II) complex under protic conditions, and its formation correlates with an ability to promote direct strand scission of DNA by phosphoribose oxidation.[76] In a complementary study, the copper(I) analogue of **5** was exposed to O_2 at low temperature in nitrile solvents and found to produce a μ-hydroperoxo dicopper(II) species $[Cu^{II}_2(PD'O^-)(^-OOH)]^{2+}$ (Scheme 3)[55] This species is capable of oxidizing the nitrile solvent[55] and may also be responsible for oxidation of guanine described in the current investigation.

An alternative bis species, $(Cu^{II}-OOH)_2$ (Scheme 3), was formed by reaction of **5** and H_2O_2.[77] This pair of mononuclear $Cu^{II}-OOH$ species is not likely to be a good oxidant because of an unfavorable O−O cleavage process.[78,79] Consistent with these predictions, no reaction of DNA was detected after

Scheme 3

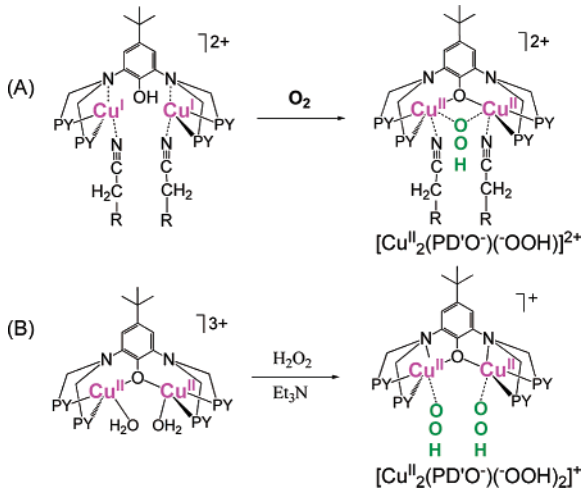

Scheme 4

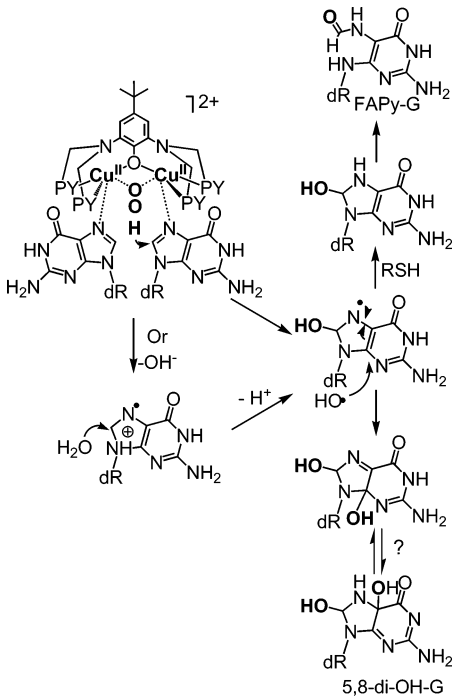

treatment with **5** and H_2O_2 (10 mM) in place of MPA/O_2 (see the Supporting Information, Figure S18).[29] The formation of mononuclear $Cu^{II}-OOH$ species may also explain the lack of reactivity observed for the mononuclear analogue of **5**. Such poor reactivity may be overcome by bridging the hydroperoxo species between two coppers, such as in $[Cu^{II}_2(PD'O^-)(^-OOH)]^{2+}$ (Scheme 3).[55]

Thus, the unique reactivity of **5** in the presence of MPA/O_2 appears to derive from the initial generation of Cu^{I}_2/O_2 (and not **5**/H_2O_2) and subsequent generation of a hydroperoxide species $[Cu^{II}_2(PD'O^-)(^-OOH)]^{2+}$ that coordinates to two guanine residues (Scheme 4). The Cu^{II}_2-OOH complex may either add a hydroxy radical directly to the guanine C8 position or extract an electron from guanine to generate the guanine radical cation. Hydration of this radical cation would also led to the same intermediate as direct hydroxy radical addition.[80] Reduction of these intermediates by a hydrogen atom (or proton-coupled electron transfer) in the presence

(72) Karlin, K. D.; Kaderli, S.; Zuberbuhler, A. D. *Acc. Chem. Res.* **1997**, *30*, 139−147.
(73) Mirica, L. M.; Ottenwaelder, X.; Stack, T. D. P. *Chem. Rev.* **2004**, *104*, 1013−1045.
(74) Lewis, E. A.; Tolman, W. B. *Chem. Rev.* **2004**, *104*, 1047−1076.
(75) Karlin, K. D.; Lee, D. H.; Kaderli, S.; Zuberbuhler, A. D. *Chem. Commun.* **1997**, 475−476.
(76) Thyagarajan, S.; Murthy, N. N.; Karlin, K. D.; Rokita, S. E. *J. Am. Chem. Soc.* **2006**, *128*, 7003−7008.
(77) Li, L.; Sarjeant, A. A.; Karlin, K. D. *Inorg. Chem.* **2006**, accepted for publication, pending minor revision.
(78) Evans, J. P.; Ahn, K.; Klinman, J. P. *J. Biol. Chem.* **2003**, *278*, 49691−49698.
(79) Chen, P.; Solomon, E. I. *J. Am. Chem. Soc.* **2004**, *126*, 4991−5000.

of excess MPA and ring-opening can yield the observed FAPy-G product. The minor +34 amu product may form concurrently by the addition of a second OH radical (or equivalent) to the hydroxylated intermediate.

Summary and Conclusions

By employing a phenolate-containing binucleating ligand PD′OH, we synthesized a dinuclear copper complex $[Cu^{II}_2(PD'O^-)(H_2O)]^{3+}$ (**5**) and characterized it structurally and spectroscopically. This complex promoted selective oxidation of guanine residues at ss/ds junctions in the presence of MPA and O_2. The reaction was most efficient when a minimum of two Gs flanked each of the 3′- and 5′-extensions from the duplex junction. Both target recognition and reaction selectivity (guanine oxidation) are likely controlled by the ligand environment of PD′OH that supports multiple coordination to guanine and formation of an end-on hydroperoxo dicopper(II) complex. The exact nature of the Cu_2O_2 species stabilized by individual multinuclear copper complexes appears critical for the type of DNA oxidation it promotes. In a complementary manner, DNA may be used to probe the reactivity of metal oxo and hydroperoxy species under nearly physiological conditions on the basis of the abundance of information available on DNA oxidation.

(80) Kasai, H.; Yamaizumi, A.; Berger, M.; Cadet, J. *J. Am. Chem. Soc.* **1992**, *114*, 9692−9694.

Acknowledgment. We thank Professor Mark M. Greenberg at the Johns Hopkins University for helpful suggestions and discussions. This work was supported by the NIH (GM28962 to K.D.K. and GM47531 to S.E.R.). We are also very grateful to Dr. Amy A. Narducci Sarjeant for help in assembling and generating X-ray data and figures.

Note Added after Print: Due to production error, there were two mistakes in equations on p 7146 in the version posted on the Web August 10, 2006 (ASAP), and published in the September 4, 2006, issue (Vol. 45, No. 18, pp 7144−7159). The correct electronic version of the paper was published on October 5, 2006, and an Addition & Correction appears in the October 30, 2006 issue (Vol. 45, No. 22).

Supporting Information Available: ORTEP views with full labeling of the cationic portions of structures, crystallographic data, and structure refinement information for complexes **5**−**9**, X-band EPR spectra of complexes **6** and **8**, autoradiograms of sequence variants of OD1A/OD2A in reactions with complex **5**, strand scission in the presence of different reductants and standard radical scavengers, and cleavage mediated by **6**/MPA/O_2 or **5**/H_2O_2. This material is available free of charge via the Internet at http://pubs.acs.org.

IC0605930